HHS Public Access

Author manuscript

Cell Rep. Author manuscript; available in PMC 2022 January 05.

Published in final edited form as:

Cell Rep. 2021 December 21; 37(12): 110147. doi:10.1016/j.celrep.2021.110147.

Thiol-based functional mimicry of phosphorylation of the two-component system response regulator ArcA promotes pathogenesis in enteric pathogens

Yitian Zhou[1], **Qinqin Pu**[1], **Jiandong Chen**[1], **Guijuan Hao**[1], **Rong Gao**[2], **Afsar Ali**[3], **Ansel Hsiao**[4], **Ann M. Stock**[2], **Mark Goulian**[5], **Jun Zhu**[1,6,*]

[1]Department of Microbiology, Perelman School of Medicine, University of Pennsylvania, Philadelphia, PA 19104, USA

[2]Center for Advanced Biotechnology and Medicine, Department of Biochemistry and Molecular Biology, Rutgers University-Robert Wood Johnson Medical School, Piscataway, NJ 08854, USA

[3]Department of Environmental and Global Health, College of Public Health and Health Professions and Emerging Pathogens Institute, University of Florida, Gainesville, FL 32610, USA

[4]Department of Microbiology & Plant Pathology, University of California, Riverside, Riverside, CA 92521, USA

[5]Department of Biology, University of Pennsylvania, Philadelphia, PA 19104, USA

[6]Lead contact

SUMMARY

Pathogenic bacteria can rapidly respond to stresses such as reactive oxygen species (ROS) using reversible redox-sensitive oxidation of cysteine thiol (-SH) groups in regulators. Here, we use proteomics to profile reversible ROS-induced thiol oxidation in *Vibrio cholerae*, the etiologic agent of cholera, and identify two modified cysteines in ArcA, a regulator of global carbon oxidation that is phosphorylated and activated under low oxygen. ROS abolishes ArcA phosphorylation but induces the formation of an intramolecular disulfide bond that promotes ArcA-ArcA interactions and sustains activity. ArcA cysteines are oxidized in cholera patient stools, and ArcA thiol oxidation drives *in vitro* ROS resistance, colonization of ROS-rich guts, and environmental survival. In other pathogens, such as *Salmonella enterica*, oxidation of conserved cysteines of ArcA orthologs also promotes ROS resistance, suggesting a common role for ROS-

*Correspondence: junzhu@pennmedicine.upenn.edu.

AUTHOR CONTRIBUTIONS

Y.Z. and J.Z. conceived and performed the experiments, analyzed the data, and wrote the manuscript. Q.P., J.C., and G.H. performed the experiments, analyzed the data, and revised the manuscript. R.G., A.A., A.H., A.S., and M.G. interpreted the results and wrote the manuscript.

SUPPLEMENTAL INFORMATION

Supplemental information can be found online at https://doi.org/10.1016/j.celrep.2021.110147.

DECLARATION OF INTERESTS

The authors declare no competing interests.

induced ArcA thiol oxidation in modulating ArcA activity, allowing for a balance of expression of stress- and pathogenesis-related genetic programs.

Graphical abstract

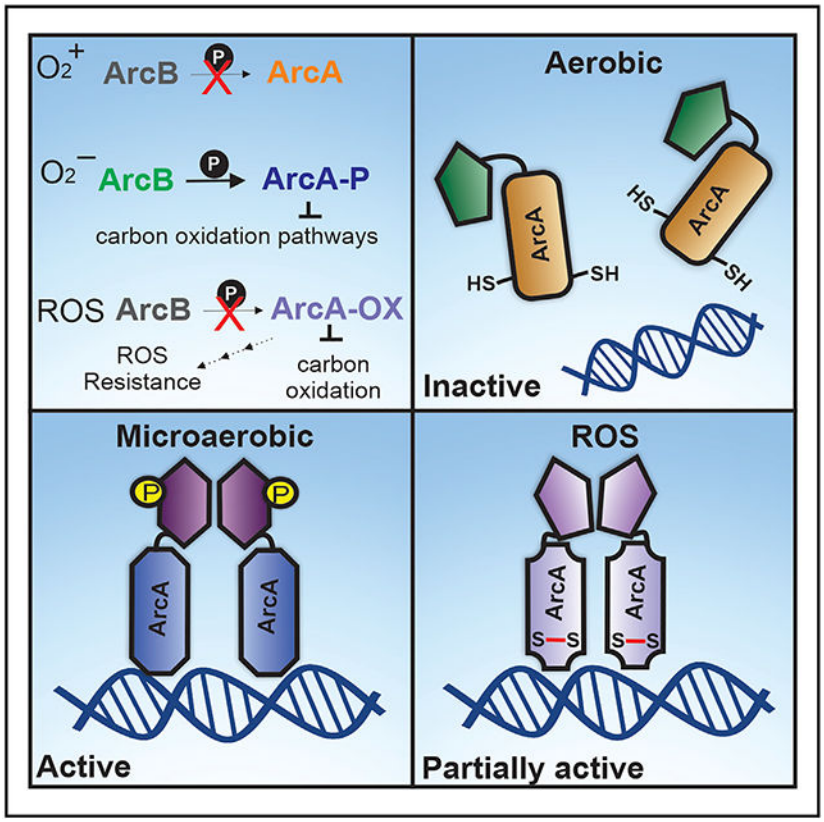

In brief

Zhou et al. perform a proteomic study of ROS-exposed *V. cholerae* and identify cysteine oxidation of the redox-sensing response regulator ArcA, which leads to sustained ArcA activity by forming intramolecular disulfide bonds. This ArcA thiol response is important for pathogenesis of *V. cholerae* and other enteric pathogens.

INTRODUCTION

Microbes show an exquisite regulatory flexibility to enable adaptation to fluctuating conditions. The ability to swiftly respond to varied environments is essential for pathogenic bacteria, which often must be able to survive not only in varied environmental reservoirs but also in the host where exclusionary effects are mediated by the immune system. To cope with new conditions, bacteria use signal transduction pathways to couple extracellular signals to specific intracellular responses. One of the most prevalent prokaryotic signaling strategies is based on two-component systems (TCSs), with a core consisting of two modular components: the membrane-bound sensor histidine kinase that senses the external stimuli and catalyzes adenosine triphosphate (ATP)-dependent autophosphorylation of a

specific histidine residue and the cytosolic response regulator that catalyzes transfer of the phosphoryl group to one of its own aspartic acid residues, which activates function, often transcriptional regulatory activities (Laub and Goulian, 2007; West and Stock, 2001).

TCSs in bacteria are involved in regulating diverse processes, such as metabolism, osmoregulation, and chemotaxis and, in the case of pathogens, expression of virulence genes and other functions important for pathogenesis (Groisman, 2016). For example, the ArcAB (aerobic respiratory control) system, where ArcA is a response regulator and ArcB is a sensor kinase, is involved in redox regulation. Under aerobic conditions, ArcB kinase activity is silenced, maintaining ArcA largely in the inactive, unphosphorylated state. Under anoxic growth conditions, ArcA is activated through reversible phosphorylation by ArcB, whose kinase activity is controlled by the redox states of the ubiquinone and menaquinone pools (Iuchi and Lin, 1992; (Malpica et al., 2004)). Following phosphorylation, ArcA acts predominantly as a global repressor of non-fermentative carbon oxidation pathways and directly activates a set of genes with a diversity of functions (Park et al., 2013). ArcA also regulates other important cellular functions, such as stress responses and DNA replication (Lee et al., 2001; Mika and Hengge, 2005). In addition, ArcA is implicated in resistance to reactive oxygen species (ROS) in pathogenic bacteria *Escherichia coli*, *Salmonella*, and *Haemophilus influenzae* (Loui et al., 2009; Lu et al., 2002; Wong et al., 2007), but the exact mechanism is not clear.

Bacterial pathogens encounter ROS that threatens to disrupt redox homeostasis as a consequence of aerobic growth or as an oxidative burst produced by the host during infections (Imlay, 2013). Bacteria have developed exquisitely tuned systems to sense these stresses and to prompt responses that allow survival and propagation under ROS insult. ROS induces thiol modifications of highly reactive cysteine residues in diverse regulatory proteins, which trigger conformational changes and activate or inactivate the transcriptional regulator (Fang et al., 2016; Vázquez-Torres, 2012). As a consequence, specific detoxification pathways are activated to mitigate ROS. For example, ROS induces intramolecular disulfide formation in the redox-sensing regulator OxyR in *E. coli* and activates a number of ROS scavenging pathways (Kim et al., 2002; Zheng et al., 1998).

Pathogens of the human gastrointestinal tract must all balance aerobic environmental lifestyles with the particular stresses of host interaction in the gut, which is microaerobic to anaerobic from the stomach onward but characterized by bursts of ROS generated in response to infection. *Vibrio cholerae*, the agent of the pandemic disease cholera, resides in both aquatic environments and human intestines (Hsiao and Zhu, 2020; Nelson et al., 2009) and can cope with harsh conditions during the transition into the host gut and subsequent expansion. For example, following infection, *V. cholerae* senses host signals and coordinates both virulence gene activation and repression to evade host defenses and successfully colonize intestines (Cakar et al., 2018; Hsiao et al., 2006; Liu et al., 2008; Yang et al., 2013), while late in infection, *V. cholerae* modulates its genetic regulatory programs to allow for dissemination into the aquatic environment (Kamp et al., 2013; Schild et al., 2007). *V. cholerae* encounters oxidative stress at early and later stages of infection, as demonstrated by an increase in ROS levels and a decrease in the levels of host antioxidant enzymes during *V. cholerae*-induced diarrhea (Bhattacharyya et al., 2004; Ellis et al., 2015).

It has been reported that OxyR, OhrR, and the virulence regulator AphB tightly regulate the expression of genes encoding catalases, peroxiredoxin, and organic hydroperoxide resistance protein, which are important for *V. cholerae* ROS resistance ((Liu et al., 2016b); (Liu et al., 2016a); Wang et al., 2012). In this study, we profiled the *V. cholerae* proteome for reversible thiol oxidation during exposure to oxidative stress. We found that cysteine residues in the response regulator ArcA were oxidized during ROS exposure. We further demonstrated that although ROS abolished ArcA phosphorylation, it promoted intramolecular disulfide formation between ArcA cysteine residues, leading to the maintenance of ArcA activity and bacterial survival during ROS challenges both *in vitro* and *in vivo*. Furthermore, we show that the function of ArcA thiol oxidation is conserved among other enteric pathogens, suggesting a general role for this ROS response system for gut-associated bacteria.

RESULTS

Proteomic profiling of *V. cholerae* reveals reversible thiol oxidation during exposure to oxidative stress

When cells are exposed to oxidative stress, cysteine residues in proteins are common targets of oxidation, leading to the formation of sulfenic acid (SOH) derivatives or mixed disulfides bonds. These reactions often serve as regulatory switches in enzymatic reactions and in the regulation of transcription (Paget and Buttner, 2003; Poole and Nelson, 2008). We wondered whether protein cysteine modification plays a role in regulation of *V. cholerae* ROS resistance. We modified a protocol that labels cysteine residues with iodoacetyl isobaric tandem mass tags (iodoTMT) (Shakir et al., 2017) to identify reversible *V. cholerae* protein oxidation in the presence of ROS (Figure 1A). We grew *V. cholerae* under the virulence-inducing condition (AKI medium) (Iwanaga and Yamamoto, 1985) and treated cells with the oxidizing agent cumene hydroperoxide (CHP). Compared with the untreated cultures, CHP treatment significantly increased protein thiol oxidation, as indicated by the decreased amount of free thiols quantified by Ellman's assays (Ellman, 1959) for sulfhydryl groups (Figure S1). The reduced thiols in extracts were blocked with *N*-ethylmaleimide (NEM). The efficiency of NEM blocking was high, as virtually no free thiols were detected after the reactions (Figure S1). Following reduction of reversibly oxidized thiols, proteins were labeled with iodoTMTzero. After digestion by trypsin, peptides were captured by an anti-TMT resin. The eluted labeled peptides were then analyzed by liquid chromatography-tandem mass spectrometry (LC-MS/MS). Using this method, we identified 373 proteins containing cysteine oxidation following exposure to ROS, including a number of ROS resistance proteins, such as AhpC, GrxA, OhrA, and thiore-doxins (Figure 1B; Data S1). We also detected a number of secreted and membrane-bound proteins that have been reported to form disulfide bonds, such as TcpA (Peek and Taylor, 1992), TcpP (Yang et al., 2013), and cholera toxin subunit B (Yu et al., 1992). The cysteine oxidation in these proteins is likely independent of ROS. The detailed *V. cholerae* cysteine oxidation proteome was subjected to another study, but here interestingly, we identified cysteine oxidation of the response regulator ArcA (Georgellis et al., 2001a). ArcA contains two cysteine residues, C173 and C233, and the peptide containing C173-TMT was detected (Figure 1C). In this study, we further investigated the relationship between cysteine oxidation and ArcA function.

ArcA thiol oxidation during ROS challenges and during human infection

To investigate the roles of ArcA cysteine residues in *V. cholerae* physiology, we generated an *arcA*-null mutant in El Tor biotype C6706. We then integrated the wild-type *arcA* ($arcA^{WT}$) or *arcA* cysteine-to-serine variants ($arcA^{C173S}$ and $arcA^{C233S}$) with the native *arcA* promoter into the *lacZ* locus in the *ΔarcA* mutant background. We first confirmed our proteomics results for ArcA. We performed a similar experiment with different labeling of oxidized thiols, allowing for visualization of thiol oxidation in a gel. Briefly, *V. cholerae* cell lysates from ROS-challenged cultures were treated with NEM, reduced with dithiothreitol (DTT), and then labeled with poly(ethylene glycol) methyl ether maleimide (PEG-Mal). PEG-Mal (2 kDa) reacts with free thiols on proteins, and the resulting PEGylated proteins can be detected by an increase in molecular weight through western blotting analyses (Figure 2A). We found that compared with the untreated culture, ArcA from the wild-type cell lysates that were treated with CHP had an approximately 4-kDa increase in size on a sodium dodecyl sulfate-polyacrylamide gel electrophoresis (SDS-PAGE) gel (Figure 2B). However, when treated with ROS, ArcA mutants that contain only one cysteine residue (C173S and C233S) displayed smaller increases in size, whereas ArcA double cysteine mutants did not change size (Figure 2B). These data suggest that both cysteine residues are indeed reversibly modified following ROS exposure. We speculate that we did not detect the ArcA C233 modification because the FC^{233}GDLED C-terminal peptide may not ionize well, as it is not a typical tryptic peptide with a terminal lysine or arginine that would yield a good positive charge.

It has been shown that during the later stages of human cholera infection, host ROS levels are elevated, and host antioxidant enzyme levels are decreased (Bhattacharyya et al., 2004; Ellis et al., 2015). We hypothesized that if *V. cholerae* experiences ROS during human infection, cysteine residues in ArcA proteins may be oxidized. To test this, we extracted total proteins from stool samples of two cholera patients in Haiti (H2627, H2629). The same labeling procedure (Figure 2A) was used. We found that when labeled with PEG-Mal, the molecular weight of *V. cholerae* ArcA in both stool samples of cholera patients increased on an SDS-PAGE gel (Figure 2C). As a comparison, we grew the strains isolated from these stool samples *in vitro* with or without CHP treatment. We found that ArcA in these strains was only modified following ROS challenge. Taken together, these data suggest that thiol oxidation occurs in ArcA during infection of human intestines.

ArcA cysteine residues are important for ArcA regulatory functions and ROS resistance

One of the typical properties of an *arcA*-null mutant in many bacteria is its sensitivity to certain dyes, such as toluidine blue (luchi and Lin, 1988). We found that the El Tor Δ*arcA* mutant was over 1,000-fold more sensitive to toluidine blue than wild type (Figure 3A), similar to the Δ*arcA* mutant in the classical biotype of *V. cholerae* (Sengupta et al., 2003). Complementation of $arcA^{WT}$ and $arcA^{C173S}$ in the Δ*arcA* mutant restored toluidine blue resistance, while addition of $arcA^{C233S}$ could not (Figure 3A). Of note, the exact mechanism behind ArcA-mediated toluidine blue resistance is not clear. ROS formation may not be the main cause for the Δ*arcA* dye phenotype (Alvarez et al., 2010). We then examined whether cysteine mutants of ArcA affect bacterial growth under different levels of oxygen availability. We found that compared with that of wild type, both Δ*arcA* and $arcA^{C233S}$

mutants, but not *arcA*^{C173S} mutants, displayed growth defects under both aerobic (Figure S2A) and microaerobic conditions (Figure S2B). Taken together, these data suggest that the ArcA^{C173S} mutation behaves like wild type under the growth conditions tested above, but the ArcA^{C233S} mutation disrupts ArcA function. We thus focused on the *arcA*^{C173S} mutant to further study the effects of thiol oxidation on ArcA activity.

As ArcA cysteine residues were reversibly oxidized following ROS insults, we then examined how ArcA thiol oxidation affects *V. cholerae* ROS resistance. Under microaerobic conditions, the *arcA*^{C173S} mutant, but not the *arcA*-null and *arcA*^{C233S} mutants, grew similar to the wild type (Figure 3B; Figure S2C). However, all three mutants were significantly more sensitive to CHP treatment (Figure 3B; Figure S2C), suggesting that cysteine oxidation of ArcA is important for ROS resistance. ArcA cysteine oxidation was also important for *V. cholerae* resistance to H_2O_2, but the effect was less prominent than that of CHP (Figure S2D). As the organic hydroperoxide-resistance protein OhrA is responsible for CHP resistance in *V. cholerae* (Liu et al., 2016a), we then examined whether *ohrA* expression is regulated by ArcA. We found that in wild type, *ohrA* expression was induced by CHP (Figure 3C), as we have shown before (Liu et al., 2016a). However, *ohrA* induction by CHP was diminished in the *arcA*^{C173S} mutant (Figure 3C), suggesting that ArcA thiol oxidation is important for *ohrA* activation and thus ROS resistance. We scanned the *ohrA* promoter region for possible ArcA-binding sites reported by a comparative genomic analysis (Ravcheev et al., 2007) and identified a putative weak ArcA box (Figure S3A); however, purified ArcA proteins, phosphorylated or oxidized, failed to bind the *ohrA* promoter DNA (Figure S3B), suggesting that ArcA regulation of *ohrA* may be indirect.

In *E. coli*, during anaerobic growth, ArcA is phosphorylated and active, whereas under aerobic conditions, ArcA is not phosphorylated due to the inactivation of ArcB kinase (Malpica et al., 2004). We thus examined how exposure to ROS affects ArcA phosphorylation in *V. cholerae* using Phos-tag SDS-PAGE and subsequent western blotting (Barbieri and Stock, 2008). We overexpressed a hexahistidine (His6)-tagged ArcA in *V. cholerae* to facilitate detection. The recombinant ArcA is functional as it could complement the growth defect of *ΔarcA* mutants (Figure S3C). Figure 4A shows that when *V. cholerae* was cultured microaerobically, but not aerobically, ArcA phosphorylation was detected, similar to that in *E. coli*. However, ArcA phosphorylation was abolished when microaerobic cultures were exposed to CHP (Figure 4A, lane 3). As a control, the conserved ArcA phosphorylation site D54 (Park and Kiley, 2014) was mutated to alanine (ArcA^{D54A}). No ArcA phosphorylation was detected in this mutant (Figure 4A), which had similar sensitivity toward toluidine blue as the *arcA*-null mutant (Figure S3D). These data suggest that ROS inhibits ArcA phosphorylation.

In light of the inhibitory effects of ROS on ArcA phosphorylation, we next examined how ROS affects the expression of ArcA-regulated genes, beginning with *sdhC* expression. SdhC (succinate dehydrogenase) is a key tricarboxylic acid (TCA) cycle enzyme and is known to be directly repressed by phosphorylated ArcA in *E. coli* (Park et al., 2013). In *V. cholerae*, the *sdhC* promoter contains a predicted ArcA-binding site (Ravcheev et al., 2007). By examining an *sdhC-lacZ* reporter, we found that under microaerobic conditions, *sdhC* expression was low in *arcA*^{WT} and *arcA*^{C173S} backgrounds but high

in the Δ*arcA* and *arcA*^{C233S} mutant (Figure 4B). However, following exposure to CHP, ArcA^{WT} could still repress *sdhC* expression, but the ArcA^{C173S} mutant failed to do so (Figure 4B, filled bars). These data suggest that although ArcA phosphorylation is inhibited following exposure to ROS (Figure 4A), ArcA regulatory functions are retained, and this is dependent on the ability of thiol oxidation of ArcA. To further support this finding, we performed electrophoretic mobility shift assays (EMSAs) using purified ArcA proteins and *sdhC* promoter DNA. As expected, when they were phosphorylated using carbamoyl phosphate, both ArcA^{WT} and ArcA^{C173S} proteins could bind to *sdhC* promoter DNA, whereas unphosphorylated, reduced forms could not (Figure 4C). We found that after treatment with CHP, ArcA^{WT} could bind DNA without phosphorylation, but ArcA^{C173S} could not (Figure 4C). However, ArcA^{D54A} mutant proteins could not bind *sdhC* DNA under the phosphorylation condition, but, once oxidized, ArcA^{D54A} was active (Figure 4C, right). Interestingly, ArcA$^{C173S/C233S}$ double cysteine mutants displayed no binding activity, and phosphorylated ArcA^{C233S} mutant proteins bound *sdhC* (Figure 4C), even though *arcA*^{C233S} mutants behaved as *arcA*-null mutants in *V. cholerae* cells. It is possible that protein folding and/or protein dosage may be different *in vitro* and in the cytosol. Taken together, these data demonstrate that ArcA binding of its target DNA can be activated via cysteine oxidation independently of phosphorylation.

ROS-induced intramolecular disulfide bond formation is critical for ArcA phosphorylation-independent activity

To further investigate how thiol oxidation promotes ArcA activity when cells are under ROS insults, we examined how thiol oxidation affects ArcA-ArcA interactions. It has been reported that phosphorylation leads to ArcA multimerization in *E. coli* (Jeon et al., 2001; Toro-Roman et al., 2005). To examine if phosphorylation and oxidation impact ArcA interactions, we used a bacterial two-hybrid assay based on split adenylyl cyclase (Karimova et al., 1998). We constructed translational fusions of *V. cholerae* ArcA wild type or C173S mutations with T25 and T18, two fragments of the catalytic domain of the *Bordetella pertussis* adenylate cyclase (CyaA) that require physical proximity to produce cyclic adenosine monophosphate (cAMP). The resulting increase in cAMP levels is detected through expression of β-galactosidase from the *lac* promoter. We found that when the strain expressing T18-ArcA^{WT} and T25-ArcA^{WT} was grown microaerobically, β-galactosidase activity was significantly higher than that observed when T25-ArcA^{WT} was grown aerobically (Figure 5A). LacZ activity in the strain expressing T18-ArcA^{C173S} and T25-ArcA^{C173S} was also higher during microaerobic growth (Figure 5A). As controls, LacZ activity from aerobic- and microaerobic-grown cultures was similar in the strains carrying the leucine zipper domains from a yeast transcription factor (GCN4) and the negative control with stand-alone T18 or T25 domains of CyaA (Figure S4A). As ArcA becomes phosphorylated under low-oxygen conditions (Malpica et al., 2004) (Figure 4A), our results suggest that phosphorylation promotes ArcA-ArcA interaction under microaerobic conditions and that ArcA C173 does not affect phosphorylation-mediated ArcA-ArcA interactions. When cells grown aerobically were exposed to CHP, however, elevated ArcA^{WT}-ArcA^{WT} interactions were observed, as ROS induced an approximately 7-fold increase in β-galactosidase activity compared with untreated cells (Figure 5B). Importantly, ROS exposure did not increase ArcA^{C173S}-ArcA^{C173S} interactions (Figure 5B).

Similarly, addition of CHP did not affect GCN4 interactions (Figure S4B). Additionally, neither $ArcA^{D54A}$-$ArcA^{D54A}$ nor $ArcA^{C233S}$-$ArcA^{C233S}$ displayed any LacZ activity under the tested conditions (Figures S4A and S4B). It is possible that these mutations in the fusion constructs happen to lock the ArcA variant in an unresponsive conformation. Taken together, these data suggest that ROS exposure promotes ArcA-ArcA interaction in the absence of phosphorylation. This interaction relies on the cysteine residues, further indicating that phosphorylation and cysteine oxidation are two post-translational modifications capable of activating ArcA regulatory functions.

We wondered what molecular mechanism drives the increase in ArcA-ArcA interactions during ROS exposure. Because cysteine oxidation often leads to disulfide bond formation, we assessed whether ArcA forms disulfide bonds in cells and, if so, whether it forms intra- or inter-molecular disulfide bonds. We grew *V. cholerae* harboring His6-tagged ArcA variants to mid-log phase, and we then treated the cultures with or without CHP. We then extracted protein and analyzed the His6-ArcA protein profiles by immunoblotting following non-reducing SDS-PAGE. These analyses were performed with or without the addition of the reductant β-mercaptoethanol (BME) to distinguish between ArcA species that had and had not formed disulfide bonds. Intermolecular disulfide bonds produce cross-linked protein oligomers, and a protein with an intramolecular disulfide bond displays increased gel mobility (Bardwell et al., 1991). Under reducing conditions (without CHP treatment), all ArcA variants displayed mobility consistent with a reduced monomer (labeled R-M in Figure 5C). When *V. cholerae* was treated with CHP, the majority of $ArcA^{WT}$ showed increased mobility, which is consistent with an oxidized monomer (labeled O-M) and suggests that ArcA forms an intramolecular disulfide bond between C173 and C233. A small fraction of $ArcA^{WT}$ formed oxidized dimers (O-D). CHP exposure induced intermolecular disulfide bond-mediated dimers in $ArcA^{C173S}$ but very little in $ArcA^{C233S}$, suggesting that intermolecular disulfide bonds mainly form between C233 residues. Because $ArcA^{C173S}$ was not active during ROS exposure in *V. cholerae* cells, these disulfide bond-mediated dimers may not be functional. Addition of the reducing agent BME in protein samples abrogated all oxidized species (Figure 5C).

We then performed additional experiments to confirm that ROS promotes ArcA to form intramolecular disulfide bonds between C173 and C233 residues. First, we treated purified $ArcA^{WT}$ and derivatives with CHP. We electrophoresed different ArcA proteins on a non-reducing SDS-PAGE gel, and we found that the oxidized forms of both $ArcA^{WT}$ and $ArcA^{D54A}$ migrated slightly faster than their reduced forms, whereas no faster migration bands were observed in the oxidized cysteine mutant ArcA (Figure S4C), corroborating the above results from *V. cholerae* whole-cell lysates in supporting the hypothesis that ROS induces intramolecular disulfide bond formation between C173 and C233. To further ascertain that C173 and C233 were involved in intramolecular disulfide formation, we subjected the oxidized ArcA to tryptic digestion followed by MS analysis. We detected a peak with a mass-to-charge ratio (*m/z*) corresponding to that of the disulfide-linked peptides consisting of $ALLHFC^{173}ENPGK$ and $FC^{233}GDLED$ (Figure 5D). These data indicate that when oxidized *in vitro*, ArcA C173 and C233 form an intramolecular disulfide bond.

Based on these results, we propose the following working model (Figure 5E). Under aerobic conditions, ArcA is not phosphorylated and does not dimerize. Phosphorylation of ArcA under microaerobic conditions promotes ArcA-ArcA interaction and ArcA activity. When *V. cholerae* is exposed to ROS, ArcA phosphorylation is inhibited, but intramolecular disulfide bonds in ArcA are formed, which may mimic the conformation of ArcA phosphorylation and lead to ArcA-ArcA interactions and DNA binding.

ArcA thiol modification is important for *V. cholerae* pathogenesis and environmental survival

Next, we investigated the roles of ArcA cysteine oxidation in *V. cholerae* pathogenesis. We first compared colonization of *ΔarcA*, *arcA*^{C173S}, and *arcA*^{C233S} mutants with wild type in an infant mouse model. We found that both *ΔarcA* and *arcA*^{C233S}, but not *arcA*^{C173S}, mutants had slight defects in colonization (Figure S5A). As *V. cholerae* experiences limited ROS insults in infant mice (Stern et al., 2012), we then performed colonization assays in a streptomycin-treated adult mouse model in which bacteria experience host-generated oxidative stresses (Spees et al., 2013; Stern et al., 2012; Wang et al., 2018). In this model, *arcA*^{C173S} mutants displayed a severe colonization defect (Figure 6A, left). In mice treated with *N*-acetyl cysteine (NAC), an antioxidant widely used in human and animal studies to artificially reduce ROS levels (Amrouche-Mekkioui and Djerdjouri, 2012; (Liu et al., 2016a)), however, *arcA*^{C173S} mutants could colonize almost as well as wild type (Figure 6A, right). In addition, *ΔarcA* and *arcA*^{C233S} colonized poorly in adult mice, and NAC treatment partially restored their colonization (Figure S5B). These data suggest that ArcA thiol oxidation is critical for *V. cholerae* survival in the ROS-rich gut.

As *V. cholerae* is a water-borne pathogen, survival in aquatic environments is a vital aspect of its life cycle. It has been demonstrated that *V. cholerae* expresses a set of genes before exiting the host intestinal tract that are advantageous for subsequent life in pond water (Schild et al., 2007). We therefore tested whether ArcA cysteine oxidation is also important for *V. cholerae* survival in aquatic environments. We first grew wild type and the *arcA*^{C173S} mutant under virulence-inducing conditions to mimic infection. We then exposed *V. cholerae* to local pond water for up to 10 days. We found that the viability of *arcA*^{C173S} mutants in the pond water was significantly reduced after 8 days (Figure 6B). These data suggest that the ability of ArcA cysteine to respond to oxidation is important for *V. cholerae* environmental survival.

ArcA thiol oxidation in other enteric pathogens

The ArcAB TCS is a major oxygen-sensing signal transduction system, regulating lifestyle transitions in many facultative anaerobic proteobacteria. In many human pathogens, such as *E. coli*, *Salmonella*, and *Klebsiella*, the ArcA cysteines C173 and C233 are conserved (Figure 7A). In many bacteria that do not have a part of their life cycle in a host environment, such as *Shewanella*, ArcA C173 is not conserved. These observations imply that ArcA cysteines in other enteric pathogens may perform similar functions to those described here for *V. cholerae*.

To test the above hypothesis, we constructed a *ΔarcA* mutant in *Salmonella enterica* serovar Typhimurium SL1344. Plasmids expressing *Salmonella arcA*^{WT} or *arcA*^{C173S} from its native promoter were introduced into *Salmonella ΔarcA* mutants. These *Salmonella* strains were grown microaerobically to mid-log phase and challenged by CHP. We found that *arcA*^{C173S} mutants showed a similarly reduced survival to that of *ΔarcA* mutants (Figure 7B). To examine whether cysteine oxidation of ArcA is important for *Salmonella* intracellular survival, we challenged the human monocytic cell line THP-1 with different *Salmonella* strains and quantified the intracellular bacteria by immunofluorescence staining. Figure 7C (top) and Figure 7D (left) show that, on average, six wild-type *Salmonella* bacteria survived in one THP-1 cell, whereas the number of intracellular *ΔarcA* mutants was significantly reduced. Complementation of *arcA*^{WT}, but not *arcA*^{C173S}, on a plasmid restored *ΔarcA* intracellular survival. When THP-1 cells were treated with NAC, an antioxidant and scavenger of ROS (Rowe et al., 2020), however, intracellular growth of Δ*arcA* and *arcA*^{C173S} was similar to that of wild-type *Salmonella* (Figure 7C, bottom, and Figure 7D, right). Similar phenotypes were also observed when *Salmonella* strains infected Caco-2 cells (Figure S6). These results suggest that ArcA cysteine residues are important for protecting *Salmonella* from host ROS-mediated killing.

DISCUSSION

Phosphotransfer-mediated TCS pathways are widely used in bacteria to allow cells to sense and respond to environmental stimuli. In these pathways, response regulators, with a conserved N-terminal receiver domain (REC) and a variable C-terminal domain, often a DNA-binding domain (DBD), function as phosphorylation-activated switches that control regulatory outputs. The regulatory strategy is simple and versatile. REC domains exist in equilibrium between at least two conformational states. Phosphorylation stabilizes an “active” conformation of the REC domain, promoting altered domain interactions that enable effector domain function. Numerous different regulatory mechanisms based on altered domain interactions, such as disruption of inhibitory interactions between REC and effector domains or promotion of REC domain dimerization, have been documented for different response regulators (Gao et al., 2019).

In this study of *V. cholerae* ArcA, we have identified a second switch located in the DBD that is redox regulated. We found that following ROS attacks, phosphorylation of ArcA is abolished, but ArcA activity is retained because of thiol oxidation that creates an intramolecular disulfide bond between C173 and C233. A homology model of the winged helix DBD of ArcA (Figure S7) indicates that C173 and C233 are located in close proximity, with a distance of 8.5 Å between α carbons. The different redox states of the cysteines in ArcA presumably create two distinct conformations of the DBD, allowing different domain interactions that affect DNA-binding activity. One possible mechanism for activation would be disruption of an inhibitory REC-DBD interface in the disulfide-containing conformation, freeing REC domains to dimerize and/or allowing DBD domains to interact with DNA. However, because structures of full-length ArcA have not been determined, REC domain and DBD interactions in either inactive or active states are unknown, precluding a specific mechanistic understanding of how cysteines in the DBDs might alter REC-DBD interactions to regulate ArcA activity. Like the phosphorylation-regulated switch of the REC domain that

uses diverse regulatory strategies, the regulatory principle for the redox switch of the DBD can be versatile. The range of different mechanisms is illustrated by the redox regulation of *Staphylococcus aureus* response regulator AgrA, in which formation of an intramolecular disulfide bond in the DBD inactivates the response regulator by disrupting DNA binding (Sun et al., 2012), providing a regulatory strategy opposite to that of ArcA, in which disulfide bond formation enhances DNA binding. Because ArcA C173S mutants still retain a small amount of activity following ROS exposure (Figures 3C and 4B), an alternative hypothesis is that C233 oxidation to SOH is responsible for a conformational change in ArcA, and the subsequent formation of a disulfide bond with C173 may stabilize the protein in the oxidized conformation, similar to that of OxyR in *E. coli* (Helmann, 2002; Kullik et al., 1995).

In *E. coli* and other enteric bacteria, ArcA is a critical global regulator in maintaining homeostasis of redox carriers under oxygen-limiting conditions. When ArcA is phosphorylated, ArcA actively represses the expression of oxygen-requiring pathways, including the TCA cycle (including genes such as *sdhC*) and the aerobic cytochrome oxidase genes. ArcA~P is also required for proper expression of certain catabolic genes for pyruvate utilization and sugar fermentation (luchi and Lin, 1993; Park and Kiley, 2014; Salmon et al., 2005). Here, we found that although ROS may abolish ArcA phosphorylation, thiol oxidation sustains ArcA functionality, and oxidized ArcA not only activates genes responsible for bacterial survival under ROS insults (Figure 3C) but also represses genes (such as genes for respiration) normally repressed by ArcA~P (Figure 4B). These results suggest that post-translational modification of protein thiols is not just a footprint of oxidative damage but may serve as a redox regulation mechanism.

Cysteine oxidation is a common strategy for redox-mediated regulation of gene expression (Antelmann and Helmann, 2011; Sevilla et al., 2019). In TCSs, it is often the histidine kinase that is the locus for such regulation. Interestingly, in the ArcAB pathway, disulfide bond formation is involved in regulation of the activity of the histidine kinase ArcB. Quinone:quinol pools and oxygen availability dictate the redox state of cysteines in ArcB (Bekker et al., 2010; Georgellis et al., 2001b; van Beilen and Hellingwerf, 2016). Under aerobic conditions (and presumably under ROS attacks), intermolecular disulfide bonds (C180-C180 and C241-C241) between PAS domains of ArcB stabilize a dimer conformation that inhibits autophosphorylation and activates phosphatase activity of ArcB, leading to dephosphorylation and inactivation of ArcA (Malpica et al., 2004; Peña-Sandoval et al., 2005). However, we have shown that ROS-mediated oxidation of cysteines in ArcA forms an intramolecular disulfide bond in the DBD, bypassing the need for ArcB-mediated phosphorylation in an apparent paradox. The small-molecule mediators of cysteine oxidation for ArcA and ArcB are distinct, raising the possibility that the inhibition of ArcB and activation of ArcA might be specific to particular conditions, allowing for fine-tuning of response output. For example, if anaerobically growing cells encounter high cytoplasmic ROS, disulfide bond formation in the DBD would allow ArcA to temporally maintain activation of fermentative pathways and repression of respiratory pathways despite the downregulation of ArcB phosphorylation. The physiological rationale for the opposing regulatory effects of cysteine oxidation on the histidine kinase and response regulator components of the ArcAB pathway is puzzling. We have found that disulfide bond

formation in ArcA is important for *V. cholerae* pathogenesis in ROS-rich mouse intestines but not in ROS-mitigated guts. It has been reported that *Salmonella* adapts to ROS challenges by shifting redox balance to fermentation, thus diverting electrons away from the respiratory chain (Chakraborty et al., 2020). We speculate that oxidized ArcA by ROS may play a similar role. In addition, because during oxidative stress oxidized ArcA is able to continue repressing the expression of iron-sulfur cluster-containing enzymes, such as nicotinamide adenine dinucleotide (NADH):quinone oxidoreductase (Shalel-Levanon et al., 2005), succinate:quinone oxidoreductase (Iuchi and Lin, 1988), and hydrogenase 2 (Richard et al., 1999), it may help bacterial cells maintain iron homeostasis and limit Fenton chemistry. It has been shown that under ROS attacks, overproduction of enzymes containing labile iron-sulfur clusters increased the free iron content in cells and led to DNA damage (Keyer and Imlay, 1996).

We have previously shown that *V. cholerae* uses a thiol-based switch mechanism in the key virulence regulator AphB to activate virulence genes and modulate ROS resistance ((Liu et al., 2016b); (Liu et al., 2016a); Liu et al., 2011). In bacteria, thiol-based regulatory switches play central roles in cellular stress responses, particularly oxidative stresses, due to the reduction potential of protein sulfhydryls (Antelmann and Helmann, 2011; Paget and Buttner, 2003). Examples include SsrB in *Salmonella* (Husain et al., 2010), OxyR in *E. coli* (Choi et al., 2001), OhrR in *Bacillus subtilis* (Fuangthong and Helmann, 2002), and MgrA, SarZ, and AgrA in *S. aureus* (Chen et al., 2006; Chen et al., 2009; Sun et al., 2012), many of which are regulators for ROS resistance and are also involved in virulence (Chen et al., 2011). These findings suggest that bacteria may use thiol-based switch mechanisms to finely balance the expression of stress-related and pathogenesis-related genetic programs.

LIMITATIONS OF THE STUDY

Our study has several limitations. The proteomic approaches we used are not designed to quantify the degree of thiol oxidation, and the cysteine modifications we detected may not result from exposure to oxidative stress. Some membrane proteins form disulfide bonds in the absence of ROS. Multiplexing labeling will be performed to compare *V. cholerae* proteome thiol oxidation with and without ROS. In addition, although we could indirectly detect ArcA oxidation in *V. cholerae* cells of cholera patient stool samples, unfortunately, we were unable to perform a proteomic study directly on the stool samples. Finally, the exact mechanism of ArcA oxidation promoting ArcA activity is not known due to lack of a complete set of ArcA crystal structures. However, even if we could obtain oxidized ArcA crystal structures, there would be concerns that conformations or oxidation states captured as a snapshot in a crystal structure may only reflect allowable states amenable to crystal packing rather than the predominant states that exist in solution.

STAR★METHODS

RESOURCE AVAILABILITY

Lead contact—Further information and requests for resources and reagents should be directed to and will be fulfilled by the lead contact, Jun (Jay) Zhu (junzhu@pennmedicine.upenn.edu).

Materials availability

- All unique/stable reagents generated in this study, including bacterial strains and plasmids, are available from the lead contact with a completed materials transfer agreement.

Data and code availability

- The mass spectrometry proteomics data have been deposited into the MassIVE (https://massive.ucsd.edu/ProteoSAFe/static/massive.jsp) and ProteomeXchange (http://www.proteomexchange.org) data repository and are publicly available as of the date of publication. Accession numbers are listed in the key resources table. Original western blot images and microscopy data reported in this paper will be shared by the lead contact upon request.
- This paper does not report original code.
- Any additional information required to reanalyze the data reported in this paper is available from the lead contact upon request.

EXPERIMENTAL MODEL AND SUBJECT DETAILS

Bacterial strains, plasmids, and culture conditions—*V. cholerae* El Tor C6706 (Joelsson et al., 2006) was used as the parental strain in this study and were propagated in LB media containing appropriate antibiotics at 37°C, unless otherwise noted. The *arcA* deletion was constructed by cloning the regions flanking *arcA* and a kanamycin resistance cassette into the suicide vector pWM91 containing a *sacB* counter-selectable marker (Metcalf et al., 1996). The resulting plasmid was introduced into *V. cholerae* by conjugation and deletion mutants were selected for double homologous recombination events. Chromosomal complementation of *arcA*, *arcA* cysteine-to-serine variants, and $arcA^{D54A}$ mutation, was constructed by inserting *arcA* and its variants into the *lacZ* locus using pJL1 (Liu et al., 2011). The His_6-*arcA* (wild-type and cysteine mutant variants) overexpression plasmid was constructed by cloning *arcA* coding sequences into pET41 (EMD Biosciences). The plasmid harboring a P_{BAD}-controlled T7 RNA polymerase gene, pTARA (Wycuff and Matthews, 2000), was introduced into *V. cholerae* to express T7-controlled His_6-ArcA and derivatives. P_{sdhC}-*lacZ* transcriptional reporter was constructed by cloning the *sdhC* promoter DNA into pAH6 (Hsiao et al., 2009). AKI medium was used to induce virulence gene expression (Iwanaga et al., 1986). *ΔarcA* of *S. enterica* serovar Typhimurium SL1344 was constructed by the λ-red recombineering approach (Datsenko and Wanner, 2000). For complementation, *Salmonella* $arcA^{WT}$ *or* $arcA^{C173S}$ with its native promoter was cloned into pACYC117 (Chang and Cohen, 1978) and transformed into SL1344 Δ*arcA*.

Mouse models—All animal experiments were performed in strict accordance with the animal protocols that were approved by the IACUC of the University of Pennsylvania.

The streptomycin-treated adult mouse model was used to examine *V. cholerae* ROS resistance *in vivo* as previously described (Wang et al., 2018). Briefly, six-week-old female CD-1 mice were provided with drinking water with or without antioxidant N-acetyl cysteine

(NAC) [1% (wt/vol)] for one week. 0.5% (wt/vol) streptomycin and 0.5% aspartame were then added to the drinking water for the remainder of the experiment. Two days after streptomycin treatment, approximately 10^8 CFU of each of the two differentially-labeled strains (wild-type *lacZ*$^+$ and mutant l*acZ*$^-$) were mixed at a 1:1 ratio and intragastrically administered to each mouse. Fecal pellets were collected from each mouse at the indicated time points, resuspended in LB, serially diluted, and then plated on plates containing 5-bromo-4-chloro-3-indolyl-β-D-galactopyranoside (X-gal). The competitive index was calculated as the ratio of mutant to wild-type colonies normalized to the input ratio.

The infant mouse colonization assays were performed as previously described (Zhu and Mekalanos, 2003). 10^5 wild-type (*lacZ* $^+$) and mutants (*lacZ* $^-$) were mixed in a 1:1 ratio and intragastrically inoculated into 5-day-old CD-1 suckling mice (both male and female). After a 12-hr period of incubation, mice were sacrificed. Small intestines were harvested and homogenized, the ratio of mutants to wild-type bacteria was determined by plating on LB agar containing antibiotics and X-Gal.

METHOD DETAILS

Proteomic profiling of reversible thiol oxidation—Iodoacetyl isobaric tandem mass tags (iodoTMT) labeling of oxidized thiols was performed as described in (Shakir et al., 2017) and by the manufacturer's protocol (ThermoFisher, Waltham, MA) with modifications. Briefly, *V. cholerae* were grown in the AKI medium without shaking for 4 hr and then challenged with 50 μM CHP for 1 hr. The cell lysates were first incubated with 100 mM N-ethylmaleimide (NEM) and then reduced with 5 mM tris(2-carboxyethyl)phosphine (TCEP). Proteins containing reduced thiols were then labeled with iodoTMTzero and digested with trypsin (8 μg trypsin/100 μg proteins). IodoTMTzero-labeled peptides were enriched by using the Anti-TMT Resin and eluted by TMT elution buffer. The eluted peptides were submitted to the Proteomics Core at the Wistar Institute. Liquid chromatography tandem mass spectrometry (LC-MS/MS) analysis was performed using a Q Exactive HF mass spectrometer (Thermo Scientific) coupled with an UltiMate 3000 nano UPLC system (Thermo Scientific). Peptide sequences were identified using MaxQuant 1.6.8.0 (Cox and Mann, 2008). MS/MS spectra were searched against a UniProt *V. cholerae* protein database and a common contaminants database using full tryptic specificity with up to two missed cleavages. Variable modifications included in the search were an addition mass of TMTzero (324.216141) on cysteine. Consensus identification lists were generated with false discovery rates set at 1% for protein, peptide, and site identifications. To confirm the intramolecular disulfide bond formation of oxidized ArcA, the purified His_6-ArcA was treated with 10x access of CHP at 37°C for 1 hr and was separated on a non-reducing SDS-PAGE. The ArcA protein slice was trypsin digested and the resulting peptides were subjected to multidimensional liquid chromatography analysis by Taplin Mass Spectrometry Facility at Harvard University. The MS/MS scans were collected in high resolution in the Orbitrap Velos Pro ion-trap mass spectrometer (Thermo Fisher Scientific, Waltham, MA).

Determination of ArcA cysteine oxidation states *in vitro* and in cholera patient samples—*V. cholerae* wild-type and mutant *arcA* derivatives were grown in the AKI medium without shaking for 4 hr and then challenged with or without 50 μM CHP for 1 hr.

Cell pellets were resuspended in a lysis buffer containing 250 mM Tris-Cl (pH 7.5), 6M urea and 1% SDS. Rice-watery stool sample (56-ml) from suspected cholera patient admitted in different cholera treatment centers (CTCs) in Haiti was collected in stool container (Thermo Scientific). The samples were brought (within 2 h post collection) to University of Florida Field Laboratory located in Christianville, Haiti for further processing. Using standard microbiological assay (Alam et al., 2015) we determined the counts (cfu/ml) of *V. cholerae* in each stool sample. All stool samples were collected using University of Florida authorized IRBs, including IRB201800568 (detection and characterization of diarrheal pathogens in Haiti) and IRB201601821 (cholera persistence, transmission, and clinical illness in Haiti and cholera transmission and evolution in Port-au-Prince, Haiti).1 mL rice-water stool was precipitated by trichloroacetic acid and resuspended in the lysis buffer. The cell lysates were first incubated with 100 mM NEM. Reversible oxidized thiols were then reduced by 20 mM DTT and labeled with or without 10 mM poly(ethylene glycol) methyl ether maleimide (PEG-Mal, 2 kDa). Samples were applied to SDS-PAGE and western blot analysis was performed by using anti-ArcA antibody generated for *E. coli* ArcA (Park et al., 2013).

Quantification of free thiols using Ellman's reagent (DTNB)—*V. cholerae* cell lysates were precipitated by trichloroacetic acid (TCA). When indicated, protein samples were treated NEM and/or TCEP. Total proteins were acetone precipitated and rinsed to remove excess reductants. Protein samples were resuspended in 6 M urea, 0.1 M sodium phosphate, pH 8, and 0.1% SDS. Samples were then added to DTNB solution containing 0.2 mM 5,5′-dithio-bis-(2-nitrobenzoic acid) (DTNB), 0.1M sodium phosphate, pH 8.0, 1mM EDTA. The optical absorbance of the reactions was measured at 412 nm. The -SH concentration was determined based on a cysteine standard curve.

Electrophoretic mobility shift assays (EMSA)—His_6-$ArcA^{WT}$ and His_6-$ArcA^{C173S}$ proteins were expressed and purified on nickel columns according to the manufacturer's instructions (QIAGEN). PCR products containing *sdhC* promoter region were digested and end-labeled with α-^{32}P dATP. Prior to *in vitro* modification reactions, His-tags were cleaved off by an overnight thrombin digestion with 1U thrombin per 100 μg protein at 4°C and verified by SDS-PAGE followed by Coomassie staining. *In vitro* phosphorylation was carried out with 10 μM protein with 20 mM carbamoyl phosphate in the phosphorylation buffer (50 mM Tris-Cl, pH7.5, 50 mM KCl, 20 mM $MgCl_2$, 20 mM DTT, 10 μg/ml BSA) at 37°C for 1 hr. Protein oxidation was carried out by mixing 10 μM proteins with 1 mM CHP in the oxidation buffer (50 mM Tris-Cl, pH 7, 50 mM KCl, 20 mM MgCl2, 0.1% Tween 20) and incubated at 37°C for 1 hr, which was followed by running the sample through Zeba spin desalting columns (Thermo Scientific). Binding reactions contained 0.2 μM protein with different treatments indicated and 0.1 ng of DNA in a buffer consisting of 20 mM Tris pH 7.0, 50 mM KCl, 1 mM EDTA, 5% glycerol, 50 μg/ml BSA, 1 μg/reaction calf thymus DNA, and 0.5 μg/reaction polydI/dC. After 30 mins of incubation at 25°C, samples were size fractionated using 4% polyacrylamide gels in 0.5 X TAE buffer. The radioactivity of free DNA and protein-DNA complexes was visualized using a Typhoon FLA7000 Phosphoimager (GE Healthcare).

Examining ArcA interaction using the bacterial two-hybrid system—*E. coli* BTH101(Karimova et al., 1998) containing pKT25-*arcA* and pUT18c-*arcA* (wild-type or derivatives) plasmids were inoculated into 200 μl LB medium containing appropriate antibiotics with and without 50 μM CHP in 1 mL 96-well plates. The plates were then incubated at 37°C with shaking or without shaking for 12 hr. Single-step β-galactosidase activity assays were performed (Schaefer et al., 2016b) and LacZ unit was calculated with the kinetic measurements of OD_{420} over 1 hr as the slope of the OD_{420} readings over time adjusted for the initial /OD_{600} at the first time point.

SDS-PAGE analysis of intracellular ArcA phosphorylation and oxidation—*V. cholerae* containing plasmids expressing P_{T7}-arcA^{WT} and *arcA* variants, and the T7 RNA polymerase gene (Wycuff and Matthews, 2000) were grown in the AKI medium until mid-log phase. The cultures were incubated with or without 50 μM CHP for 1 hr. Cells were pelleted and lysed by Bugbuster (EMD Millipore) and equal amount of total proteins were loaded onto Mn-based Phos-tag SDS-PAGE gels (Kinoshita et al., 2009) to detect ArcA phosphorylation, or non-reducing SDS-PAGE gels to examine ArcA oxidation. After electrophoresis, western blot analysis was performed by using anti-His_6 antibody (Rockland Immunochemicals).

***Salmonella* ROS resistance *in vitro* and during infection—**Overnight cultures of *Salmonella enterica* serovar Typhimurium SL1344 wild-type and *arcA* derivatives were inoculated at 1:40 into LB supplemented with 130 μM NaCl and appropriate antibiotics and grown standing at 37°C for 3 hr. Virulence induced cultures (Galán and Curtiss, 1990) were incubated with or without 200 μM CHP for an additional hour. Viable cells were enumerated by serial dilutions and plating.

THP-1 and Caco-2 cells were cultured in RPMI 1640 medium containing with 10% fetal bovine serum (FBS) and 1% penicillin/streptomycin. THP-1 monocytes cells were induced by phorbol 12-myristate 13-acetate (PMA) at the concentration of 50 ng/ml for 48 hr before use. Cells were maintained at 37°C with 5% CO_2 in a humidified chamber. For infection, *Salmonella* virulence induced cultures were washed with PBS and inoculated into THP-1 or Caco-2 cells with an MOI of 20 in antibiotic-free fresh FBS medium changed 1 hr prior to the infection. 30 min prior to the infection, 5 mM N-Acetyl-L-cysteine (NAC) or equal volume of PBS was added. 100 μg/ml gentamicin were added 30 mins prior to harvesting to eliminate extracellular *Salmonella*. After 6 hr of infection, cells were fixed and permeated by 4% paraformaldehyde and 0.2% Triton X-100. Followed by 10% serum blocking, the cells were stained by β-tubulin (Red) and the *Salmonella* cells were stained by anti-*Salmonella typhimurium* 0-4 antibody (1E6) (Green) with corresponding second antibodies. Nucleus were stained with DAPI (Blue). Cells and the bacteria were imaged by Leica confocal microscopy and the intracellular *Salmonella* numbers in THP-1 cells were quantified by counting 50 THP-1 cells for intracellular bacteria. For Caco-2 infection, intracellular bacterial counts were evaluated at the time indicated. Supernatant was discarded, and the adhered Caco-2 cells were washed with PBS for five times. 200 μL of 0.2% Triton X-100 in PBS was added to each well for 1 hr of incubation at room

temperature before collected in an Eppendorf tube. The resulting cell lysate is used for enumeration of CFU at respective time points. Data collected from three infection repeats.

QUANTIFICATION AND STATISTICAL ANALYSIS

Figure legends detail all quantification and statistical analyses, including number of biological repeats, animal numbers, and statistical tests. For comparisons of between two datasets, unpaired Student t test analyses were used. For comparisons of among multiple datasets, one-way ordinary ANOVA tests were used. All one-way ANOVA analyses assumed Gaussian distribution and were performed as non-parametric tests. Two-way ANOVA analyses were performed between groups. Two-way ANOVA analyses with multiple comparisons compared values within each row across columns. All statistical analyses were conducted using Graphpad Prism v9.0.2.

Supplementary Material

Refer to Web version on PubMed Central for supplementary material.

ACKNOWLEDGMENTS

We thank Drs. Fevzi Daldal, Igor Brodsky, Rahul Kohli, and Hui Wang for helpful discussions and technical support. We thank Dr. Patricia Kiley for kindly providing us with the ArcA antibody. We thank Dr. Sunny Shin for kindly providing us the mammalian cell lines. We also thank Drs. Hsin-Yao Tang and Ross Tomaino for helping with the proteomics studies. This study is supported by NIH grants AI120489 (J.Z.), AI157106 (J.Z. and A.H.), GM124724 (A.H.), GM080279 (M.G.), and GM131727 (A.M.S.).

REFERENCES

Alam MT, Weppelmann TA, Longini I, De Rochars VM, Morris JG Jr., and Ali A (2015). Increased isolation frequency of toxigenic *Vibrio cholerae* O1 from environmental monitoring sites in Haiti. PLoS ONE 10, e0124098. [PubMed: 25853552]

Alvarez AF, Malpica R, Contreras M, Escamilla E, and Georgellis D (2010). Cytochrome d but not cytochrome o rescues the toluidine blue growth sensitivity of arc mutants of *Escherichia coli*. J. Bacteriol 192, 391–399. [PubMed: 19897650]

Amrouche-Mekkioui I, and Djerdjouri B (2012). *N*-acetylcysteine improves redox status, mitochondrial dysfunction, mucin-depleted crypts and epithelial hyperplasia in dextran sulfate sodium-induced oxidative colitis in mice. Eur. J. Pharmacol 691, 209–217. [PubMed: 22732651]

Antelmann H, and Helmann JD (2011). Thiol-based redox switches and gene regulation. Antioxid. Redox Signal 14, 1049–1063. [PubMed: 20626317]

Barbieri CM, and Stock AM (2008). Universally applicable methods for monitoring response regulator aspartate phosphorylation both in vitro and in vivo using Phos-tag-based reagents. Anal. Biochem 376, 73–82. [PubMed: 18328252]

Bardwell JC, McGovern K, and Beckwith J (1991). Identification of a protein required for disulfide bond formation *in vivo*. Cell 67, 581–589. [PubMed: 1934062]

Bekker M, Alexeeva S, Laan W, Sawers G, Teixeira de Mattos J, and Hellingwerf K (2010). The ArcBA two-component system of Escherichia coli is regulated by the redox state of both the ubiquinone and the menaquinone pool. J. Bacteriol 192, 746–754. [PubMed: 19933363]

Bhattacharyya S, Ghosh S, Shant J, Ganguly NK, and Majumdar S (2004). Role of the W07-toxin on Vibrio cholerae-induced diarrhoea. Biochim. Biophys. Acta 1670, 69–80. [PubMed: 14729143]

Cakar F, Zingl FG, Moisi M, Reidl J, and Schild S (2018). *In vivo* repressed genes of *Vibrio cholerae* reveal inverse requirements of an H^+/Cl^- transporter along the gastrointestinal passage. Proc. Natl. Acad. Sci. USA 115, E2376–E2385. [PubMed: 29463743]

Chakraborty S, Liu L, Fitzsimmons L, Porwollik S, Kim JS, Desai P, McClelland M, and Vazquez-Torres A (2020). Glycolytic reprograming in *Salmonella* counters NOX2-mediated dissipation of ΔpH. Nat. Commun 11, 1783. [PubMed: 32286292]

Chang AC, and Cohen SN (1978). Construction and characterization of amplifiable multicopy DNA cloning vehicles derived from the P15A cryptic miniplasmid. J. Bacteriol 134, 1141–1156. [PubMed: 149110]

Chen PR, Bae T, Williams WA, Duguid EM, Rice PA, Schneewind O, and He C (2006).An oxidation-sensing mechanism is used by the global regulator MgrA in *Staphylococcus aureus*. Nat. Chem. Biol 2, 591–595. [PubMed: 16980961]

Chen PR, Nishida S, Poor CB, Cheng A, Bae T, Kuechenmeister L, Dunman PM, Missiakas D, and He C (2009). A new oxidative sensing and regulation pathway mediated by the MgrA homologue SarZ in *Staphylococcus aureus*. Mol. Microbiol 71, 198–211. [PubMed: 19007410]

Chen PR, Brugarolas P, and He C (2011). Redox signaling in human pathogens. Antioxid. Redox Signal 14, 1107–1118. [PubMed: 20578795]

Choi H, Kim S, Mukhopadhyay P, Cho S, Woo J, Storz G, and Ryu SE (2001). Structural basis of the redox switch in the OxyR transcription factor. Cell 105, 103–113. [PubMed: 11301006]

Cox J, and Mann M (2008). MaxQuant enables high peptide identification rates, individualized p.p.b.-range mass accuracies and proteome-wide protein quantification. Nat. Biotechnol 26, 1367–1372. [PubMed: 19029910]

Datsenko KA, and Wanner BL (2000). One-step inactivation of chromosomal genes in *Escherichia coli* K-12 using PCR products. Proc. Natl. Acad. Sci. USA 97, 6640–6645. [PubMed: 10829079]

Ellis CN, LaRocque RC, Uddin T, Krastins B, Mayo-Smith LM, Sarracino D, Karlsson EK, Rahman A, Shirin T, Bhuiyan TR, et al. (2015). Comparative proteomic analysis reveals activation of mucosal innate immune signaling pathways during cholera. Infect. Immun 83, 1089–1103. [PubMed: 25561705]

Ellman GL (1959). Tissue sulfhydryl groups. Arch. Biochem. Biophys 82, 70–77. [PubMed: 13650640]

Fang FC, Frawley ER, Tapscott T, and Vázquez-Torres A (2016). Discrimination and Integration of Stress Signals by Pathogenic Bacteria. Cell Host Microbe 20, 144–153. [PubMed: 27512902]

Fuangthong M, and Helmann JD (2002). The OhrR repressor senses organic hydroperoxides by reversible formation of a cysteine-sulfenic acid derivative. Proc. Natl. Acad. Sci. USA 99, 6690–6695. [PubMed: 11983871]

Galán JE, and Curtiss R III. (1990). Expression of *Salmonella typhimurium* genes required for invasion is regulated by changes in DNA supercoiling. Infect. Immun 58, 1879–1885. [PubMed: 2160435]

Gao R, Bouillet S, and Stock AM (2019). Structural Basis of Response Regulator Function. Annu. Rev. Microbiol 73, 175–197. [PubMed: 31100988]

Georgellis D, Kwon O, and Lin EC (2001a). Quinones as the redox signal for the arc two-component system of bacteria. Science 292, 2314–2316. [PubMed: 11423658]

Georgellis D, Kwon O, Lin EC, Wong SM, and Akerley BJ (2001b). Redox signal transduction by the ArcB sensor kinase of *Haemophilus influenzae* lacking the PAS domain. J. Bacteriol 183, 7206–7212. [PubMed: 11717280]

Groisman EA (2016). Feedback Control of Two-Component Regulatory Systems. Annu. Rev. Microbiol 70, 103–124. [PubMed: 27607549]

Helmann JD (2002). OxyR: a molecular code for redox sensing? Sci. STKE 2002, pe46. [PubMed: 12419849]

Hsiao A, and Zhu J (2020). Pathogenicity and virulence regulation of *Vibrio cholerae* at the interface of host-gut microbiome interactions. Virulence 11, 1582–1599. [PubMed: 33172314]

Hsiao A, Liu Z, Joelsson A, and Zhu J (2006). *Vibrio cholerae* virulence regulator-coordinated evasion of host immunity. Proc. Natl. Acad. Sci. USA 103, 14542–14547. [PubMed: 16983078]

Hsiao A, Xu X, Kan B, Kulkarni RV, and Zhu J (2009). Direct regulation by the *Vibrio cholerae* regulator ToxT to modulate colonization and anticolonization pilus expression. Infect. Immun 77, 1383–1388. [PubMed: 19168737]

Husain M, Jones-Carson J, Song M, McCollister BD, Bourret TJ, and Vázquez-Torres A (2010). Redox sensor SsrB Cys203 enhances *Salmonella* fitness against nitric oxide generated in the host immune response to oral infection. Proc. Natl. Acad. Sci. USA 107, 14396–14401. [PubMed: 20660761]

Imlay JA (2013). The molecular mechanisms and physiological consequences of oxidative stress: lessons from a model bacterium. Nat. Rev. Microbiol 11, 443–454. [PubMed: 23712352]

Iuchi S, and Lin EC (1988). arcA (dye), a global regulatory gene in *Escherichia coli* mediating repression of enzymes in aerobic pathways. Proc. Natl. Acad. Sci. USA 85, 1888–1892. [PubMed: 2964639]

Iuchi S, and Lin EC (1992). Purification and phosphorylation of the Arc regulatory components of *Escherichia coli*. J. Bacteriol 174, 5617–5623. [PubMed: 1512197]

Iuchi S, and Lin EC (1993). Adaptation of *Escherichia coli* to redox environments by gene expression. Mol. Microbiol 9, 9–15. [PubMed: 8412675]

Iwanaga M, and Yamamoto K (1985). New medium for the production of cholera toxin by *Vibrio cholerae* O1 biotype El Tor. J. Clin. Microbiol 22, 405–408. [PubMed: 2995438]

Iwanaga M, Yamamoto K, Higa N, Ichinose Y, Nakasone N, and Tanabe M (1986). Culture conditions for stimulating cholera toxin production by *Vibrio cholerae* O1 El Tor. Microbiol. Immunol 30, 1075–1083. [PubMed: 3543624]

Jeon Y, Lee YS, Han JS, Kim JB, and Hwang DS (2001). Multimerization of phosphorylated and non-phosphorylated ArcA is necessary for the response regulator function of the Arc two-component signal transduction system. J. Biol. Chem 276, 40873–40879. [PubMed: 11527965]

Joelsson A, Liu Z, and Zhu J (2006). Genetic and phenotypic diversity of quorum-sensing systems in clinical and environmental isolates of *Vibrio cholerae*. Infect. Immun 74, 1141–1147. [PubMed: 16428762]

Kamp HD, Patimalla-Dipali B, Lazinski DW, Wallace-Gadsden F, and Camilli A (2013). Gene fitness landscapes of *Vibrio cholerae* at important stages of its life cycle. PLoS Pathog. 9, e1003800. [PubMed: 24385900]

Karimova G, Pidoux J, Ullmann A, and Ladant D (1998). A bacterial two-hybrid system based on a reconstituted signal transduction pathway. Proc. Natl. Acad. Sci. USA 95, 5752–5756. [PubMed: 9576956]

Keyer K, and Imlay JA (1996). Superoxide accelerates DNA damage by elevating free-iron levels. Proc. Natl. Acad. Sci. USA 93, 13635–13640. [PubMed: 8942986]

Kim SO, Merchant K, Nudelman R, Beyer WF Jr., Keng T, DeAngelo J, Hausladen A, and Stamler JS (2002). OxyR: a molecular code for redox-related signaling. Cell 109, 383–396. [PubMed: 12015987]

Kinoshita E, Kinoshita-Kikuta E, and Koike T (2009). Separation and detection of large phosphoproteins using Phos-tag SDS-PAGE. Nat. Protoc 4, 1513–1521. [PubMed: 19798084]

Kullik I, Toledano MB, Tartaglia LA, and Storz G (1995). Mutational analysis of the redox-sensitive transcriptional regulator OxyR: regions important for oxidation and transcriptional activation. J. Bacteriol 177, 1275–1284. [PubMed: 7868602]

Laub MT, and Goulian M (2007). Specificity in two-component signal transduction pathways. Annu. Rev. Genet 41, 121–145. [PubMed: 18076326]

Lee YS, Han JS, Jeon Y, and Hwang DS (2001). The arc two-component signal transduction system inhibits in vitro *Escherichia coli* chromosomal initiation. J. Biol. Chem 276, 9917–9923. [PubMed: 11133990]

Liu Z, Miyashiro T, Tsou A, Hsiao A, Goulian M, and Zhu J (2008). Mucosal penetration primes *Vibrio cholerae* for host colonization by repressing quorum sensing. Proc. Natl. Acad. Sci. USA 105, 9769–9774. [PubMed: 18606988]

Liu Z, Wang H, Zhou Z, Sheng Y, Naseer N, Kan B, and Zhu J (2016a). Thiol-based switch mechanism of virulence regulator AphB modulates oxidative stress response in Vibrio cholerae. Mol. Microbiol 102, 939–949. [PubMed: 27625149]

Liu Z, Wang H, Zhou Z, Naseer N, Xiang F, Kan B, Goulian M, and Zhu J (2016b). Differential Thiol-Based Switches Jump-Start *Vibrio cholerae* Pathogenesis. Cell Rep. 14, 347–354. [PubMed: 26748713]

Liu Z, Yang M, Peterfreund GL, Tsou AM, Selamoglu N, Daldal F, Zhong Z, Kan B, and Zhu J (2011). *Vibrio cholerae* anaerobic induction of virulence gene expression is controlled by thiol-based switches of virulence regulator AphB. Proc. Natl. Acad. Sci. USA 108, 810–815. [PubMed: 21187377]

Loui C, Chang AC, and Lu S (2009). Role of the ArcAB two-component system in the resistance of *Escherichia coli* to reactive oxygen stress. BMC Microbiol. 9, 183. [PubMed: 19715602]

Lu S, Killoran PB, Fang FC, and Riley LW (2002). The global regulator ArcA controls resistance to reactive nitrogen and oxygen intermediates in *Salmonella enterica* serovar Enteritidis. Infect. Immun. 70, 451–461. [PubMed: 11796570]

Malpica R, Franco B, Rodriguez C, Kwon O, and Georgellis D (2004). Identification of a quinone-sensitive redox switch in the ArcB sensor kinase. Proc. Natl. Acad. Sci. USA 101, 13318–13323. [PubMed: 15326287]

McWilliam H, Li W, Uludag M, Squizzato S, Park YM, Buso N, Cowley AP, and Lopez R (2013). Analysis Tool Web Services from the EMBL-EBI. Nucleic Acids Res 41, W597–W600. [PubMed: 23671338]

Metcalf WW, Jiang W, Daniels LL, Kim SK, Haldimann A, and Wanner BL (1996). Conditionally replicative and conjugative plasmids carrying lacZ alpha for cloning, mutagenesis, and allele replacement in bacteria. Plasmid 35, 1–13. [PubMed: 8693022]

Mika F, and Hengge R (2005). A two-component phosphotransfer network involving ArcB, ArcA, and RssB coordinates synthesis and proteolysis of sigmaS (RpoS) in *E. coli*. Genes Dev. 19, 2770–2781. [PubMed: 16291649]

Nelson EJ, Harris JB, Morris JG Jr., Calderwood SB, and Camilli A (2009). Cholera transmission: the host, pathogen and bacteriophage dynamic. Nat. Rev. Microbiol 7, 693–702. [PubMed: 19756008]

Paget MS, and Buttner MJ (2003). Thiol-based regulatory switches. Annu. Rev. Genet 37, 91–121. [PubMed: 14616057]

Park DM, and Kiley PJ (2014). The influence of repressor DNA binding site architecture on transcriptional control. MBio 5, e01684–14. [PubMed: 25161193]

Park DM, Akhtar MS, Ansari AZ, Landick R, and Kiley PJ (2013). The bacterial response regulator ArcA uses a diverse binding site architecture to regulate carbon oxidation globally. PLoS Genet. 9, e1003839. [PubMed: 24146625]

Peek JA, and Taylor RK (1992). Characterization of a periplasmic thiol:disulfide interchange protein required for the functional maturation of secreted virulence factors of *Vibrio cholerae*. Proc. Natl. Acad. Sci. USA 89, 6210–6214. [PubMed: 1631111]

Peña-Sandoval GR, Kwon O, and Georgellis D (2005). Requirement of the receiver and phosphotransfer domains of ArcB for efficient dephosphorylation of phosphorylated ArcA *in vivo*. J. Bacteriol 187, 3267–3272. [PubMed: 15838055]

Poole LB, and Nelson KJ (2008). Discovering mechanisms of signaling-mediated cysteine oxidation. Curr. Opin. Chem. Biol 12, 18–24. [PubMed: 18282483]

Ravcheev DA, Gerasimova AV, Mironov AA, and Gelfand MS (2007). Comparative genomic analysis of regulation of anaerobic respiration in ten genomes from three families of gamma-proteobacteria (Enterobacteriaceae, Pasteurellaceae, Vibrionaceae). BMC Genomics 8, 54. [PubMed: 17313674]

Richard DJ, Sawers G, Sargent F, McWalter L, and Boxer DH (1999). Transcriptional regulation in response to oxygen and nitrate of the operons encoding the [NiFe] hydrogenases 1 and 2 of *Escherichia coli*. Microbiology (Reading) 145, 2903–2912. [PubMed: 10537212]

Rowe SE, Wagner NJ, Li L, Beam JE, Wilkinson AD, Radlinski LC, Zhang Q, Miao EA, and Conlon BP (2020). Reactive oxygen species induce antibiotic tolerance during systemic *Staphylococcus aureus* infection. Nat. Microbiol 5, 282–290. [PubMed: 31819212]

Salmon KA, Hung SP, Steffen NR, Krupp R, Baldi P, Hatfield GW, and Gunsalus RP (2005). Global gene expression profiling in *Escherichia coli* K12: effects of oxygen availability and ArcA. J. Biol. Chem 230, 15084–15096.

Schaefer J, Jovanovic G, Kotta-Loizou I, and Buck M (2016a). A data comparison between a traditional and the single-step β-galactosidase assay. Data Brief 8, 350–352. [PubMed: 27331113]

Schaefer J, Jovanovic G, Kotta-Loizou I, and Buck M (2016b). Single-step method for β-galactosidase assays in Escherichia coli using a 96-well microplate reader. Anal. Biochem 503, 56–57. [PubMed: 27036618]

Schild S, Tamayo R, Nelson EJ, Qadri F, Calderwood SB, and Camilli A (2007). Genes induced latein infection increase fitness of *Vibrio cholerae* after release into the environment. Cell Host Microbe 2, 264–277. [PubMed: 18005744]

Sengupta N, Paul K, and Chowdhury R (2003). The global regulator ArcA modulates expression of virulence factors in *Vibrio cholerae*. Infect. Immun 71, 5583–5589. [PubMed: 14500477]

Sevilla E, Bes MT, González A, Peleato ML, and Fillat MF (2019). Redox-Based Transcriptional Regulation in Prokaryotes: Revisiting Model Mechanisms. Antioxid. Redox Signal 30, 1651–1696. [PubMed: 30073850]

Shakir S, Vinh J, and Chiappetta G (2017). Quantitative analysis of the cysteine redoxome by iodoacetyl tandem mass tags. Anal. Bioanal. Chem 409, 3821–3830. [PubMed: 28389918]

Shalel-Levanon S, San KY, and Bennett GN (2005). Effect of oxygen, and ArcA and FNR regulators on the expression of genes related to the electron transfer chain and the TCA cycle in *Escherichia coli*. Metab. Eng 7, 364–374. [PubMed: 16140031]

Spees AM, Wangdi T, Lopez CA, Kingsbury DD, Xavier MN, Winter SE, Tsolis RM, and Bäumler AJ (2013). Streptomycin-induced inflammation enhances *Escherichia coli* gut colonization through nitrate respiration. MBio 4, e00430–13.

Stern AM, Hay AJ, Liu Z, Desland FA, Zhang J, Zhong Z, and Zhu J (2012). The NorR regulon is critical for *Vibrio cholerae* resistance to nitric oxide and sustained colonization ofthe intestines. MBio 3, e00013–12. [PubMed: 22511349]

Sun F, Liang H, Kong X, Xie S, Cho H, Deng X, Ji Q, Zhang H, Alvarez S, Hicks LM, et al. (2012). Quorum-sensing agr mediates bacterial oxidation response via an intramolecular disulfide redox switch in the response regulator AgrA. Proc. Natl. Acad. Sci. USA 109, 9095–9100. [PubMed: 22586129]

Toro-Roman A, Mack TR, and Stock AM (2005). Structural analysis and solution studies of the activated regulatory domain of the response regulator ArcA: a symmetric dimer mediated by the α4-β5-α5 face. J. Mol. Biol 349, 11–26. [PubMed: 15876365]

van Beilen JW, and Hellingwerf KJ (2016). All Three Endogenous Quinone Species of *Escherichia coli* Are Involved in Controlling the Activity of the Aerobic/Anaerobic Response Regulator ArcA. Front. Microbiol 7, 1339. [PubMed: 27656164]

Vázquez-Torres A (2012). Redox active thiol sensors of oxidative and nitrosative stress. Antioxid. Redox Signal 17, 1201–1214. [PubMed: 22257022]

Wang H, Chen S, Zhang J, Rothenbacher FP, Jiang T, Kan B, Zhong Z, and Zhu J (2012). Catalases promote resistance of oxidative stress in *Vibrio cholerae*. PLoS ONE 7, e53383. [PubMed: 23300923]

Wang H, Xing X, Wang J, Pang B, Liu M, Larios-Valencia J, Liu T, Liu G, Xie S, Hao G, et al. (2018). Hypermutation-induced *in vivo* oxidative stress resistance enhances *Vibrio cholerae* host adaptation. PLoS Pathog. 14, e1007413. [PubMed: 30376582]

Waterhouse A, Bertoni M, Bienert S, Studer G, Tauriello G, Gumienny R, Heer FT, de Beer TAP, Rempfer C, Bordoli L, et al. (2018). SWISS-MODEL: homology modelling of protein structures and complexes. Nucleic Acids Res 46, W296–W303. [PubMed: 29788355]

West AH, and Stock AM (2001). Histidine kinases and response regulator proteins in two-component signaling systems. Trends Biochem. Sci 26, 369–376. [PubMed: 11406410]

Wong SM, Alugupalli KR, Ram S, and Akerley BJ (2007). The ArcA regulon and oxidative stress resistance in *Haemophilus influenzae*. Mol. Microbiol 64, 1375–1390. [PubMed: 17542927]

Wycuff DR, and Matthews KS (2000). Generation of an AraC-araBAD promoter-regulated T7 expression system. Anal. Biochem 277, 67–73. [PubMed: 10610690]

Yang M, Liu Z, Hughes C, Stern AM, Wang H, Zhong Z, Kan B, Fenical W, and Zhu J (2013). Bile salt-induced intermolecular disulfide bond formation activates *Vibrio cholerae* virulence. Proc. Natl. Acad. Sci. USA 110, 2348–2353. [PubMed: 23341592]

Yu J, Webb H, and Hirst TR (1992). A homologue of the *Escherichia coli* DsbA protein involved in disulphide bond formation is required for enterotoxin biogenesis in *Vibrio cholerae*. Mol. Microbiol 6, 1949–1958. [PubMed: 1324389]

Zheng M, Aslund F, and Storz G (1998). Activation of the OxyR transcription factor by reversible disulfide bond formation. Science 279, 1718–1721. [PubMed: 9497290]

Zhu J, and Mekalanos JJ (2003). Quorum sensing-dependent biofilms enhance colonization in *Vibrio cholerae*. Dev. Cell 5, 647–656. [PubMed: 14536065]

Highlights

- Proteomic study identifies *V. cholerae* ArcA cysteine oxidation during ROS insults
- ArcA cysteine oxidation mimics ArcA phosphorylation
- ArcA cysteine oxidation is important for *V. cholerae* pathogenesis
- ArcA cysteine oxidation is conserved in other enteric pathogens

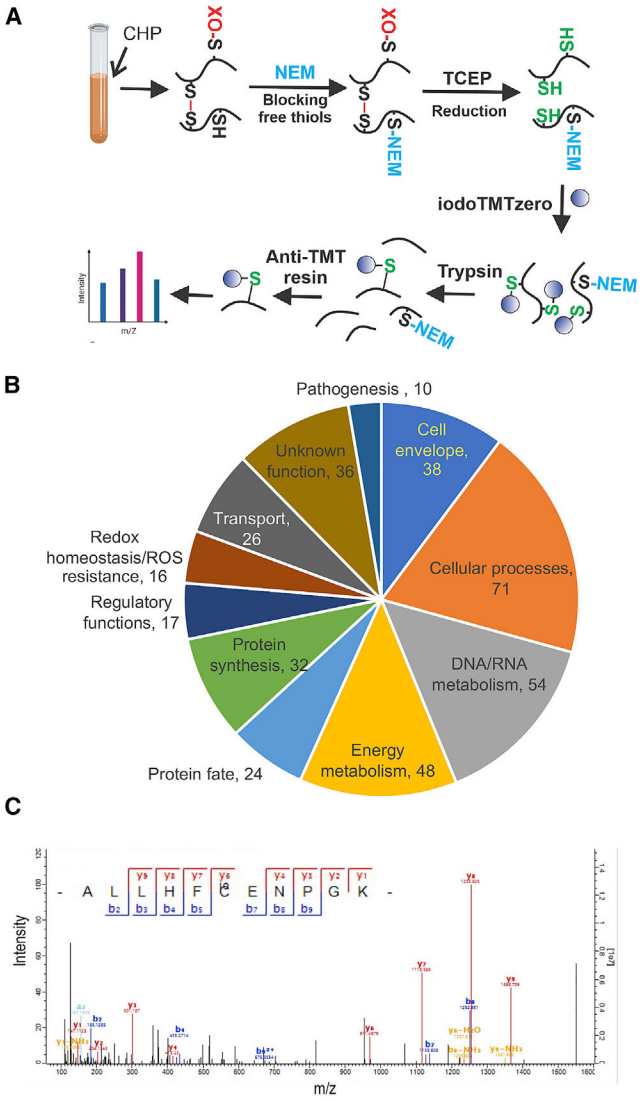

Figure 1. Profiling oxidation-sensitive cysteines in the *V. cholerae* whole proteome

(A) Schematic of the thiol labeling approach. *V. cholerae* was grown under the virulence-inducing condition and was subsequently challenged with 50 μM CHP for 1 h. Thiols in the extracts are alkylated with NEM. Following reduction of reversibly oxidized thiols, proteins were labeled with iodoTMTzero. After digestion with trypsin, peptides were captured by an anti-TMT resin. The eluted labeled peptides were then analyzed by LC-MS/MS.

(B) Pie chart showing distribution of modified cysteine-containing proteins in *V. cholerae* by protein functional categories.

(C) LC-MS/MS spectrum of ArcA peptides containing the C173 TMT modification.

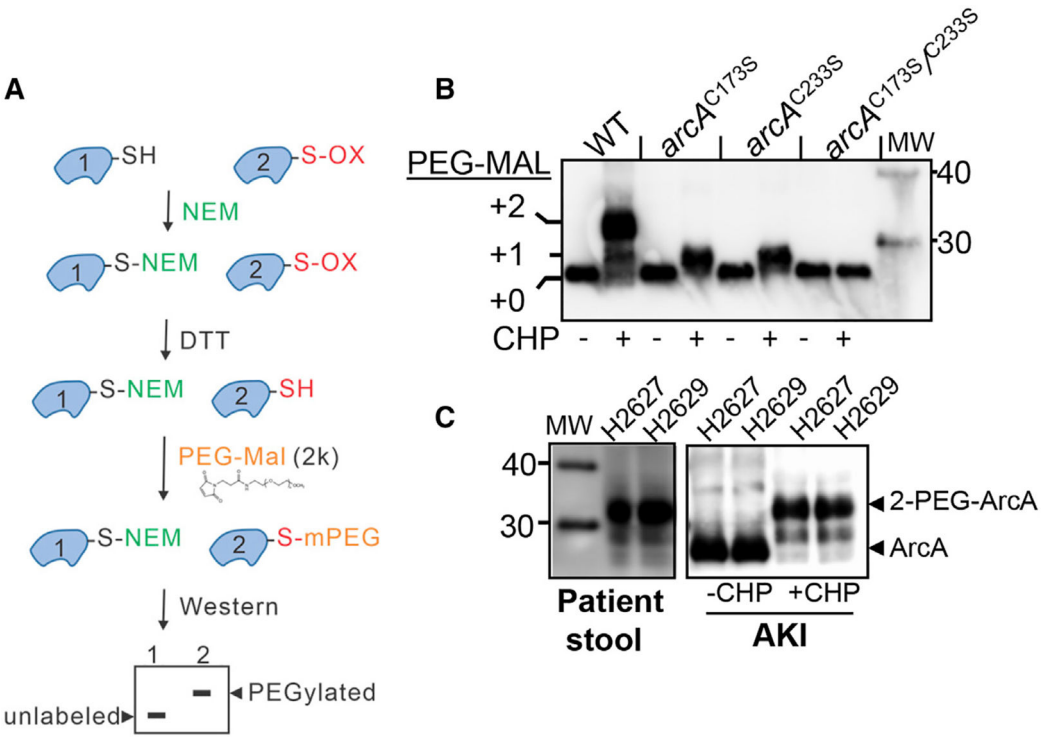

Figure 2. ArcA cysteine oxidation *in vitro* and during human infection

(A) Labeling reversible thiols by PEG-Mal. A 2-kDa increase is expected if the protein has one cysteine reversibly oxidized.

(B) Confirmation of ArcA cysteine oxidation. Free thiols in cell lysates from *V. cholerae* wild type and *arcA* mutant derivatives with or without CHP exposure were first blocked with NEM. Oxidized thiols were then reduced and labeled with PEG-Mal (2 kDa). Western blotting analysis was then performed using the anti-ArcA antibody.

(C) ArcA thiol oxidation in *V. cholerae* of cholera patient stool. Two cholera patient stool samples were precipitated and resuspended in lysis buffer. Free thiols in cell lysates were first blocked, and oxidized thiols were reduced. Samples were then treated with PEG-Mal (2 kDa). *V. cholerae* strains isolated from the stool samples were grown with and without CHP and labeled as described in (B). Western blotting analysis was then performed using the anti-ArcA antibody.

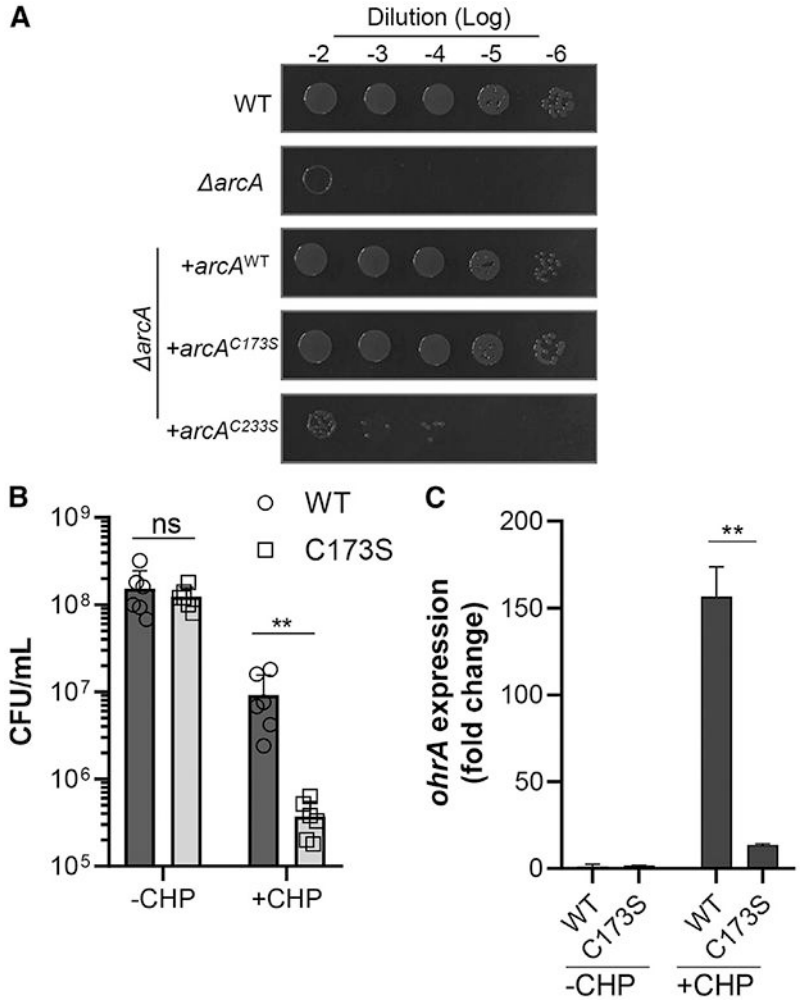

Figure 3. The effects of ArcA cysteine residues on *V. cholerae* ArcA activity and ROS resistance

(A) Toluidine blue resistance. Wild type and *arcA* variants were grown overnight on Luria-Bertani (LB) agar plates and resuspended in saline for serial dilution and spotting on LB agar plates containing 1 μg/mL toluidine blue. The plates were incubated at 37°C overnight. (B and C) Effects of the ArcA C173S mutation on ROS resistance (B) and the expression of *ohrA* (C). Wild type and *arcA*^{C173S} mutants were grown in AKI medium to mid-log phase and treated with or without 60 μM CHP for 1 h. Viable cell counts were determined by serial dilutions. RNA was also collected, and *ohrA* transcripts were quantified by quantitative PCR (qPCR). The mean of six independent assays is shown, and error bars represent the standard deviation; **, $p < 0.005$ (Student's t test); ns, no significance.

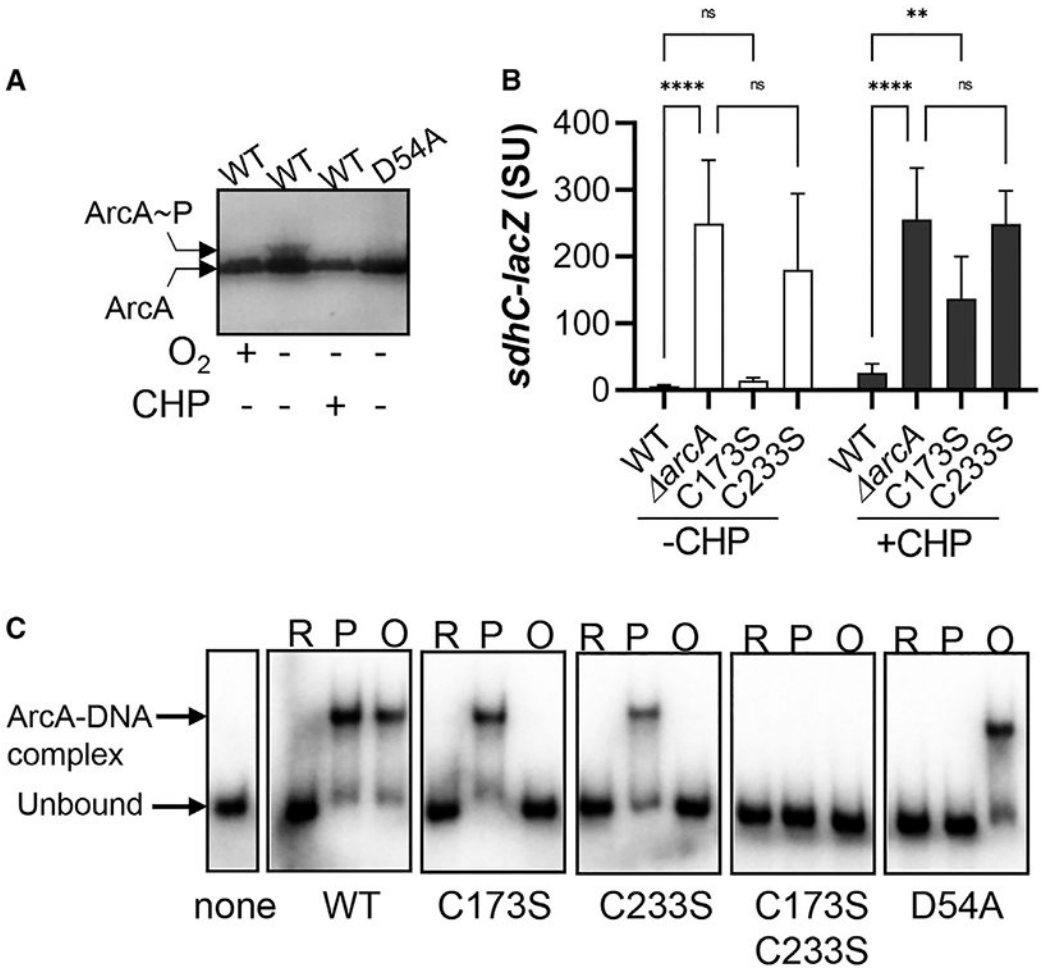

Figure 4. ROS effects on ArcA phosphorylation and activity

(A) ArcA phosphorylation. *V. cholerae* overexpressing N-terminally His-tagged ArcA^{WT} or ArcA^{D54A} were grown aerobically (O_2^+), microaerobically (O_2^-), or microaerobically in the presence of 50 μM CHP. Whole-cell lysates were analyzed by Phos-Tag gel electrophoresis followed by anti-His6 western blotting to visualize ArcA phosphorylation.

(B) ROS effects on ArcA repression of *sdhC* transcription. Wild type, Δ*arcA*, and *arcA*^{C173S} mutants containing P$_{sdhc}$-*lacZ* reporter plasmids were grown in AKI medium to mid-log phase and treated with or without 60 μM CHP for 1 h. β-Galactosidase activity was measured and normalized against viable cell numbers (SU, special units = β-gal unit/CFU × 10^6). The mean of nine datapoints from three independent assays is shown, and error bars represent the standard deviation; ****, $p < 0.0001$ (Student's t test); ns, no significance.

(C) EMSA assays. Purified ArcA wild type and ArcA-mutant derivative proteins were treated with DTT (R, reduced), carbamoyl phosphate (P, phosphorylated), and CHP (O, oxidized) before incubating with the ^{32}P-labeled *sdhC* promoter DNA. The reaction mixes were separated on a native gel and imaged on a Typhoon phosphorimager.

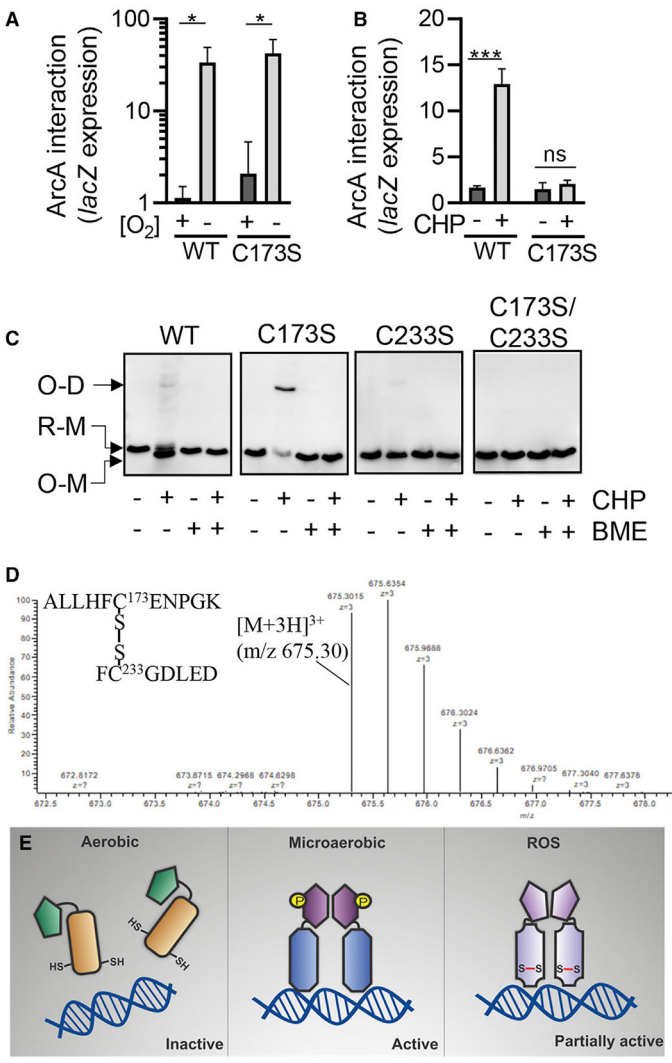

Figure 5. ArcA thiol oxidation induces intramolecular disulfide bond formation and enhances ArcA-ArcA interaction

(A and B) ArcA-ArcA interaction. *E. coli* BTH101 containing pKT25-*arcA* and pUC18c-*arcA* and derivatives were grown for 12 h at 37°C in LB aerobically or microaerobically (A) or microaerobically with or without 50 μM CHP (B). Single-step β-galactosidase activity assays were performed, and the LacZ unit was calculated by the formula described in Schaefer et al., 2016a. The mean of nine datapoints from three independent assays is shown, and error bars represent the standard deviation; ***, $p < 0.001$ (Student's t test); ns, no significance.

(C) *V. cholerae* containing overexpressed His6-tagged ArcA variants were grown under the virulence-inducing condition. When indicated, 50 μM CHP was added during ArcA induction. Cell lysates (normalized by optical density at 600 nm [OD_{600}]) with or without 100 mM BME were separated on a non-reducing 12% SDS-polyacrylamide gel followed by western blotting analysis using anti-His6 antibody; O-M, oxidized monomer; R-M, reduced monomer; O-D, oxidized dimer.

(D) Full MS spectrum of the $[M + 3H]^{3+}$ (m/z = 675.30) ions of the disulfide-linked ALLHFC^{173}ENPGK and FC^{233}GDLED.

(E) Working model. ArcA in the reduced unphosphorylated state is in an inactive form as monomers. A microaerobic environment leads ArcA phosphorylation and thus ArcA-ArcA interaction, allowing target DNA binding. When cells are challenged by ROS, ArcA phosphorylation is abolished, but an intramolecular disulfide bond is formed, introducing a conformational change that retains ArcA-ArcA interaction and DNA binding.

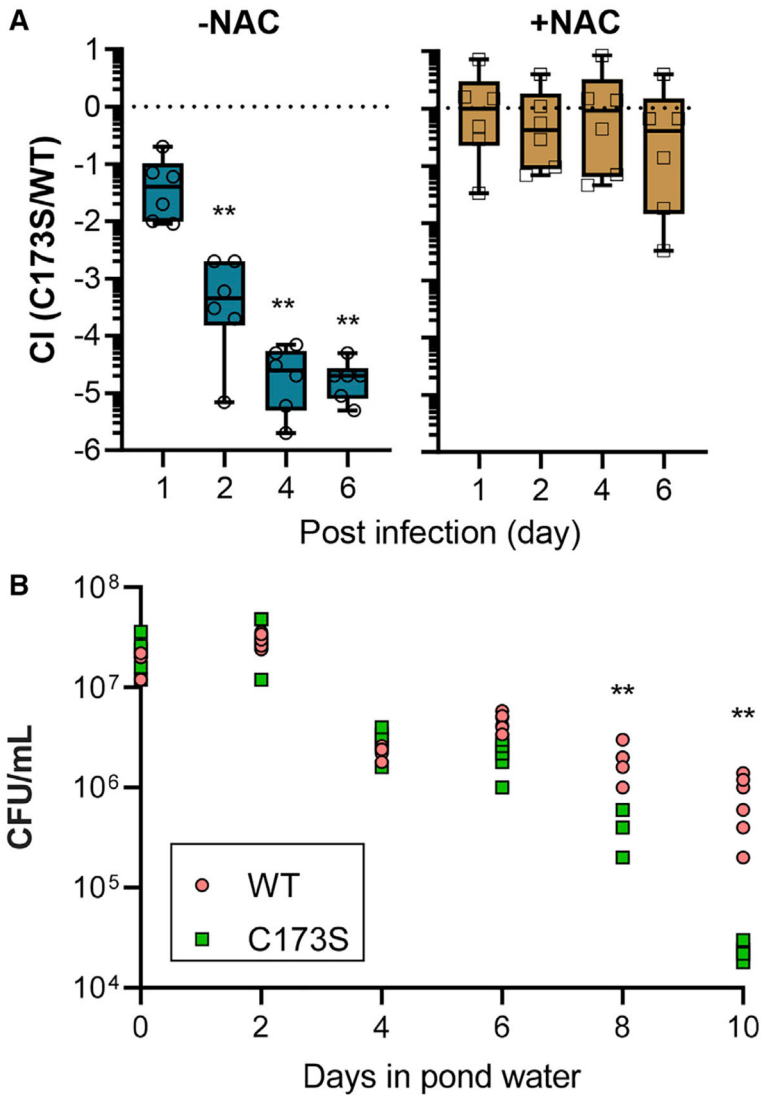

Figure 6. The involvement of ArcA thiol oxidation in *V. cholerae* pathogenesis

(A) Colonization. 10^8 cells of wild type and *arcA*^{C173S} mutants were mixed 1:1 and intragastrically administered to mice without NAC treatment (−NAC, left) and mice with NAC (+NAC, right). Fecal pellets were collected from each mouse at the indicated time points and plated onto selective plates. The competitive index (CI) was calculated as the ratio of mutant to wild-type colonies normalized to the input ratio; horizontal line, mean CI of 6 mice; **, $p < 0.005$ (Mann Whitney test).

(B) Survival in pond water. Wild type and *arcA*^{C173S} mutants were grown in AKI medium until mid-log phase. Cells were rinsed and transferred to pond water supplemented with 0.5× M9 salts (Schild et al., 2007) and incubated at room temperature with aeriation. At the time point indicated, samples were withdrawn, and viable cells were determined; **, $p < 0.005$ (Student's t test).

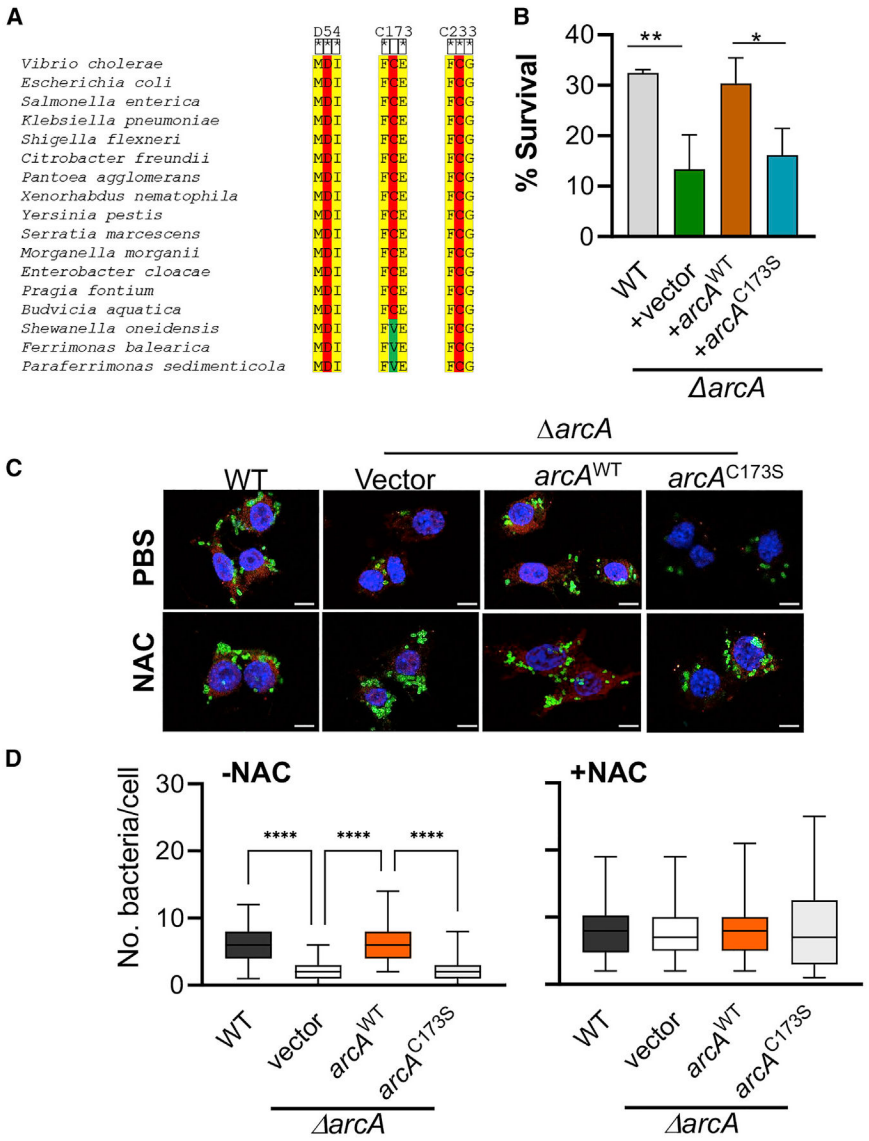

Figure 7. The importance of ArcA cysteine residues in other enteric pathogens

(A) Alignment of ArcA homolog sequences from different bacteria using Clustal O. The alignment around the phosphorylation site D54 and the two cysteine residues C173 and C233 are shown.

(B) *In vitro* ROS resistance in *Salmonella*. The indicated *Salmonella* strains were grown statically at 37°C to mid-log phase. A subset of cultures was treated with 200 μM CHP for 1 h. Viable cells were then determined. The mean of nine datapoints from three independent assays is shown, and error bars represent the standard deviation; **, $p < 0.005$; *, $p < 0.05$ (Student's t test).

(C and D) Immunofluorescence staining (C) and quantification (D) of intracellular bacteria in THP-1 cells infected by *Salmonella*. Before infection, THP-1 cells were treated with or without NAC. THP-1 cells were infected for 6 h at a multiplicity of infection (MOI) of 20. Extracellular bacteria were eliminated by gentamicin treatment. Cells were stained by β-tubulin (red), and *Salmonella* were stained by anti-*Salmonella* antibody (green). Nuclei

were stained with 4′,6-diamidino-2-phenylindole (DAPI; blue). Cells and bacteria were imaged by confocal microscopy, and the intracellular *Salmonella* number was quantified; n = 50; ****, $p < 0.0001$; ns, no significance (one-way analysis of variance [ANOVA]); scale bar, 5 μm.

KEY RESOURCES TABLE

REAGENT or RESOURCE	SOURCE	IDENTIFIER
Antibodies		
Anti-ArcA antibody	Park et al., 2013	N/A
Anti-His6 antibody	Rockland Immunochemicals	Cat# 200-301-382: RRID: AB_10703081
Anti-*Salmonella typhimurium* 0-4 antibody (1E6)	Santa Cruz Biotechnology	Cat# sc-52223; RRID: AB_630226
Anti-mouse IgG	Cell Signaling Technology	Cat# 7076S; RRID: AB_330924
Secondary antibody for anti-*Salmonella*	Santa Cruz Biotechnology	Cat# sc-516140; RRID: N/A
Tubulin antibody	Santa Cruz Biotechnology	Cat# sc-5274; RRID: AB_2288090
Bacterial and virus strains		
V. cholerae C6706 WT	Joelsson et al., 2006	N/A
V. cholerae C6706 *lacZ*	Liu et al., 2008	N/A
V. cholerae C6706 *arcA*	This work	N/A
V. cholerae C6706 *arcA lacZ::arcA*^{C173S}	This work	N/A
V. cholerae C6706 *arcA lacZ::arcA*^{C233S}	This work	N/A
V. cholerae C6706 *arcA lacZ::arcA*^{C173SC233S}	This work	N/A
V. cholerae C6706 *arcA lacZ::arcA*^{D54A}	This work	N/A
V. cholerae C6706 *arcA lacZ::arcA*^{WT}	This work	N/A
BL21(DE3) His6-ArcA^{WT} expression strain	This work	N/A
BL21(DE3) His6-ArcA^{C173S} expression strain	This work	N/A
BL21(DE3) His6-ArcA^{C233S} expression strain	This work	N/A
BL21(DE3) His6-ArcA^{C173SC233S} expression strain	This work	N/A
BL21(DE3) His6-ArcA^{D54A} expression strain	This work	N/A
BHT101 with pKT25-GCN4 and pUT18c-GCN4	Karimova et al., 1998	N/A
BHT101 with pKT25 and pUT18c vectors	Karimova et al., 1998	N/A
BTH101 ArcA^{WT}-ArcA^{WT}	This work	N/A
BTH101 ArcA^{WT}-ArcA^{C173S}	This work	N/A
T7 RNA polymerase His$_6$-ArcA^{WT} *V. cholerae* expression strain	This work	N/A
C6706 *lacZ*$^{-}$ with a P*sdhC-lacZ* reporter plasmid	This work	N/A
C6706 *arcA::kan lacZ*$^{-}$ with a P*sdhC -lacZ* reporter plasmid	This work	N/A
C6706 *arcA::kan lacZ::arcAC173S* with a P*sdhC-lacZ* reporter plasmid	This work	N/A
C6706 *arcA::kan lacZ::arcAC233S* with a P*sdhC-lacZ* reporter plasmid	This work	N/A
T7 RNA polymerase His$_6$-ArcA^{C173S} *V. cholerae* expression strain	This work	N/A
T7 RNA polymerase His$_6$-ArcA^{C233S} *V. cholerae* expression strain	This work	N/A
T7 RNA polymerase His$_6$-ArcA^{C173SC233S} *V. cholerae* expression strain	This work	N/A
Salmonella enterica serovar Typhimurium SL1344 WT	Gift from Dr. Igor Brodsky (University of Pennsylvania)	N/A

REAGENT or RESOURCE	SOURCE	IDENTIFIER
SL1344 *arcA::Kan*	This work	N/A
SL1344 *arcA::Kan* with pACYC117-P*arcA-arcA*^{WT}	This work	N/A
SL1344 *arcA::Kan* pACYC117-P*arcA-arcA*^{C173S}	This work	N/A
Biological samples		
Patient-derived stool sample H2627	University of Florida Field Laboratory located in Christianville, Haiti	IRB201800568, IRB201601821
Patient-derived stool sample H2629	University of Florida Field Laboratory located in Christianville, Haiti	IRB201800568, IRB201601821
Chemicals, peptides, and recombinant proteins		
Cumene hydroperoxide (CHP)	Alfa Aesar	L06866
Hydrogen peroxide (H_2O_2)	Sigma	H1009
Toluidine blue (TB)	Sigma	T3260
Poly(ethylene glycol) methyl ether maleimide (PEG-Mal, 2kDa)	Sigma	731765
5,5′-Dithio-bis-(2-nitrobenzoic acid), DTNB (Ellman's reagent)	Thermo Fisher	22582
DAPI	Sigma	D9542
Phorbol 12-myristate 13-acetate (PMA)	MP Biomedicals	183882
Iodoacetyl isobaric tandem mass tags (iodoTMTzero)	Thermo Fisher	90100
N-Ethylmaleimide (NEM)	Sigma	04259
Bond-Breaker TCEP solution	Thermo Fisher	77720
HEPES, 1.0M buffer soln., pH 8.0	Fisher Scientific	AAJ63578AK
Immobilized Anti-TMT Antibody Resin	Thermo Fisher	90076
TMT Elution Buffer	Thermo Fisher	90104
Ni-NTA Agarose	Qiagen	30210
Thrombin	Millipore Sigma	696713
Carbamoyl phosphate disodium salt	Santa Cruz	72461-86-0
Trypsin	Promega	V5111
RPMI 1640 medium	Corning	10-640-CM
Pen Strep antibiotics	Gibco	15140-122
Fetal bovine serum (FBS)	Corning	MT35010-CV
Bugbuster	Millipore Sigma	70584
N-Acetyl-L-cysteine (NAC)	Fisher Scientific	AAA1540914
Phos-tag™ Acrylamide	Nard	AAL-107
α P32-dATP	Perkin Elmer	BLU512H250UC
Critical commercial assays		
RNeasy Mini kit	Qiagen	74104
Turbo DNA-free kit	Ambion	AM1907
Biorad iScript cDNA synthesis kit	Biorad	170-8890
All-in-one qPCR mix	Genecopoeia	AOPR-1000
Deposited data		
Proteomic profiling of reversible thiol oxidation in *V. cholerae*	This work	MassIVE: MSV000087932; ProteomeXchange: PXD027688

REAGENT or RESOURCE	SOURCE	IDENTIFIER
Experimental models: cell lines		
Caco2	Gift from Dr. Sunny Shin (University of Pennsylvania)	N/A
THP-1	Gift from Dr. Sunny Shin (University of Pennsylvania)	N/A
Experimental models: organisms/strains		
CD-1 mouse	Charles River Laboratories	022
Oligonucleotides		
Oligos used as control and for constructing strains	See Table S1	N/A
Recombinant DNA		
pWM91-*arcA::kan*	This work	N/A
pET41-His6-ArcA^{WT}	This work	N/A
pET41-His6-ArcA^{C173S}	This work	N/A
pET41-His6-ArcA^{C173S}	This work	N/A
pET41-His6-ArcA^{C233S}	This work	N/A
pET41-His6-ArcA^{C173SC233S}	This work	N/A
pET41-His6-ArcA^{D54A}	This work	N/A
pWM91-*arcA* (VC2368)	This work	N/A
pTara	Addgene	#31491
pJL1-p*arcA*-*arcA*^{WT}	This work	N/A
pJL1-p*arcA*-*arcA*^{C173S}	This work	N/A
pJL1-p*arcA*-*arcA*^{C233S}	This work	N/A
pJL1-p*arcA*-*arcA*^{C173SC233S}	This work	N/A
pJL1-p*arcA*-*arcA*^{D54A}	This work	N/A
pAH6-p*sdhC-lacZ*	This work	N/A
pKT25-*arcA*^{WT}	This work	N/A
pKT25-*arcA*^{C173S}	This work	N/A
pKT25-*arcA*^{C233S}	This work	N/A
pKT25-*arcA*^{D54A}	This work	N/A
pUT18c-*arcA*^{WT}	This work	N/A
pUT18c-*arcA*^{C173S}	This work	N/A
pUT18c-*arcA*^{C233S}	This work	N/A
pUT18c-*arcA*^{D54A}	This work	N/A
Salmonella arcA^{WT} with native promoter	Genewiz	Fragment gene
Salmonella arcA^{C173S} with native promoter	Genewiz	Fragment gene
pACYC117-*Salmonella* p*arcA*-*arcA*^{WT}	This work	N/A
pACYC117-*Salmonella* p*arcA*-*arcA*^{C173S}	This work	N/A
Software and algorithms		
CLUSTAL O(1.2.4) multiple sequence alignment	(McWilliam et al., 2013)	https://www.ebi.ac.uk/Tools/msa/clustalo/
SWISSMODEL	(Waterhouse et al., 2018)	https://swissmodel.expasy.org